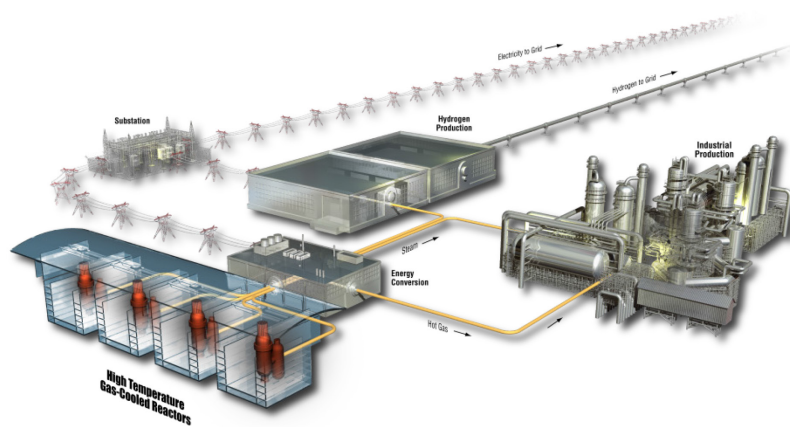


A Summary of the Results from the DOE Advanced Gas Reactor (AGR) Fuel Development and Qualification Program

David Petti, Blaise Collin,
Douglas Marshall

April 2017

The INL is a
U.S. Department of Energy
National Laboratory
operated by
Battelle Energy Alliance



DISCLAIMER

This information was prepared as an account of work sponsored by an agency of the U.S. Government. Neither the U.S. Government nor any agency thereof, nor any of their employees, makes any warranty, expressed or implied, or assumes any legal liability or responsibility for the accuracy, completeness, or usefulness, of any information, apparatus, product, or process disclosed, or represents that its use would not infringe privately owned rights. References herein to any specific commercial product, process, or service by trade name, trade mark, manufacturer, or otherwise, does not necessarily constitute or imply its endorsement, recommendation, or favoring by the U.S. Government or any agency thereof. The views and opinions of authors expressed herein do not necessarily state or reflect those of the U.S. Government or any agency thereof.

A Summary of the Results from the DOE Advanced Gas Reactor (AGR) Fuel Development and Qualification Program

April 2017

David Petti, Blaise Collin, Douglas Marshall

**Idaho National Laboratory
Idaho Falls, Idaho 83415**

<http://www.inl.gov>

**Prepared for the
U.S. Department of Energy
Office of Nuclear Energy
Under DOE Idaho Operations Office
Contract DE-AC07-05ID14517**

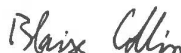
INL ART TDO Program

A Summary of the Results from the DOE Advanced Gas Reactor (AGR) Fuel Development and Qualification Program

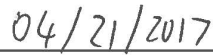
INL/EXT-16-40784
Revision 0

April 2017

Technical Reviewer: (Confirmation of mathematical accuracy, and correctness of data and appropriateness of assumptions.)



Blaise P. Collin
ART TDO TRISO Fuel



Date



Douglas W. Mitchell
ART TDO TRISO Fuel Fabrication Technical Lead



Date

Approved by:



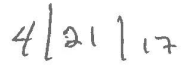
David A. Petti, Director
Nuclear Fuels and Materials Division
INL Laboratory Fellow



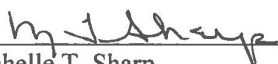
Date



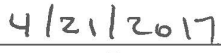
Paul A. Demkowicz
Director TRISO Fuels



Date



Michelle T. Sharp
INL Quality Engineer



Date

CONTENTS

ACRONYMS.....	ix
1. INTRODUCTION.....	1
2. FUNCTIONAL CONTAINMENT AND TRISO FUEL REQUIREMENTS.....	2
3. FABRICATION.....	3
4. IRRADIATION PERFORMANCE.....	12
4.1 AGR-1 and AGR-2.....	13
4.2 AGR-3/4.....	19
4.3 AGR-5/6/7.....	21
4.4 Uncertainty Considerations.....	24
5. POST-IRRADIATION EXAMINATION AND SAFETY TESTING.....	25
5.1 Fission Product Distributions.....	25
5.2 Irradiated Fuel Particle Microstructural Evolution.....	26
5.3 Safety Testing.....	28
5.4 SiC Failure Mechanisms.....	31
6. FUEL PERFORMANCE MODELING.....	32
7. LICENSING IMPLICATIONS.....	34
8. REFERENCES.....	34

FIGURES

Figure 1. Radar plot of key parameters for TRISO-coated fuel performance.....	2
Figure 2. Comparison of standard deviation of coating layer thicknesses from the AGR program with historic German, Japanese, and U.S. TRISO fuel.....	10
Figure 3. Comparison of heavy metal contamination, SiC defect fraction, and total leachable heavy metal for AGR-2 and development coating runs compared to historic German fuel.....	12
Figure 4. Horizontal cross section of an AGR-1 experiment capsule.....	14
Figure 5. ATR core cross section.....	15
Figure 6. AGR-1 experiment flow path.....	15
Figure 7. End-of-life Kr-85m fission gas release for AGR-1 and AGR-2 compared to historic performance in U.S. and German TRISO fuel irradiations.....	16
Figure 8. Distribution of time at temperature experienced by TRISO fuel particles in AGR-1.....	17
Figure 9. AGR-2 time at temperature for Capsules 5 and 6 (UCO fuel) (designed to operate at a time-averaged temperature of 1,250°C).....	18

Figure 10. AGR-2 time at temperature for Capsule 2 (UCO fuel) (designed to operate at a time-averaged peak temperature of 1,400°C).	18
Figure 11. Comparison of fuel temperature distribution in AGR-1 and AGR-2 capsules with that expected from a 750°C outlet temperature HTGR (the General Atomics steam cycle modular helium reactor)	19
Figure 12. Axial (left) cross-section view and schematic (right) of AGR-3/4 capsules.	20
Figure 13. Combined AGR fitted line and R/B per failed particle data for AGR irradiations, historical irradiations, and models (the blue shaded area is 95% bounds of the fitted line).....	21
Figure 14. AGR-5/6/7 capsules cross section.	23
Figure 15. AGR-5/6/7 test train in-core section.....	23
Figure 16. Range of fractional fission product inventories found in the matrix of examined compacts (red columns) and on the irradiation capsule components (blue columns). Instances where compacts and capsules contained SiC failures are indicated separately on the plot. Hashed areas indicate that the measured values on some capsule components were above the detection limit of the techniques; therefore, the sum of contributions from all components represents a conservative upper bound for the total inventory in several of the capsules.....	26
Figure 17. Examples of various AGR-1 irradiated particle microstructures (from Reference []).	27
Figure 18. Fission product release from heating of AGR-1 Compact 6-4-3 at 1,600°C.....	28
Figure 19. Cs-134 release from AGR-1 compacts heated at 1,600, 1,700, and 1,800°C.....	29
Figure 20. Ag-110m fractional release from AGR-1 compacts during safety tests. Test temperature is indicated by the color coding shown in the figure. Note the increase in release fraction for two of the 1,800°C tests (in red) after ~100 hours at 1,800°C.	30
Figure 21. Fission product release results from AGR-2 Compacts 5-2-2 and 2-2-2 under high-temperature accident heating.	31
Figure 22. (a) X-ray tomogram showing microstructure in as-irradiated Compact 5-2-3 particle that led to SiC failure and cesium release; (b) x-ray close-up of degraded pathway through SiC; and (c) scanning electron microscope micrograph of degraded region with energy dispersive x-ray spectroscopy identification of Pd and U in the SiC and Si outside the SiC.....	32

TABLES

Table 1. Allowable fuel defect levels and in-service failures.	3
Table 2. QC methods for TRISO-coated particle fuel.	4
Table 3. Evolution of fuel fabrication in AGR program.	6
Table 4. UCO and UO ₂ kernel attributes for use in AGR-2 irradiation.	7
Table 5. Properties of TRISO-coated UCO and UO ₂ particles for use in AGR-2 irradiation.....	8
Table 6. Selected properties for AGR-2 compacts.....	9

Table 7. Comparison of defects at laboratory (AGR-1) and engineering (AGR-2) scale. Fractional defect values are 95% confidence estimates based on sample size. The AGR-1 data are reported for each different fuel type: Baseline, Variant 1, Variant 2, and Variant 3 (B, V1, V2, and V3, respectively). 11

Table 8. AGR fuel program irradiation tests..... 12

Table 9. AGR-5/6/7 irradiation test specifications. 22

ACRONYMS

3D	three dimensional
AGR	advanced gas reactor
ATR	Advanced Test Reactor
BAF	bacon anisotropy factor
BWXT	BWX Technologies, Inc.
DOE	U.S. Department of Energy
DTF	designed-to-fail
EAB	Exclusion Area Boundary
FIMA	fissions per initial metal atom
GA	General Atomics
HTGR	high-temperature gas-cooled reactor
IPyC	inner pyrolytic carbon layer
LEU	low-enriched uranium
MTHM	metric tons of heavy metal
MTS	methyltrichlorosilane
NEFT	northeast flux trap
NGNP	Next Generation Nuclear Plant
OPyC	outer pyrolytic carbon layer
ORNL	Oak Ridge National Laboratory
PARFUME	PARticle FUEl ModEl
PIE	post-irradiation examination
QC	quality control
R/B	release to birth
SC-MHR	steam cycle modular helium reactor
SiC	silicon carbide
TC	thermocouples
TRISO	tristructural isotropic
UCO	uranium oxycarbide
VHTR	very high temperature reactor

A Summary of the Results from the DOE Advanced Gas Reactor (AGR) Fuel Development and Qualification Program

1. INTRODUCTION

Modular high-temperature gas-cooled reactor (HTGR) designs were developed to be safe through natural processes that prevent significant coated-particle fuel degradation and failure under all licensing basis events. The principle that guides HTGR design concepts is to passively maintain core temperatures below fission product release thresholds under all accident scenarios. The required level of fuel performance and fission product retention reduces the radioactive source term by many orders of magnitude relative to source terms for other reactor types and allows a graded approach to emergency planning and the potential elimination of the need for evacuation and sheltering beyond a small exclusion area. Achieving this level, however, is predicated on exceptionally high coated-particle fuel fabrication quality and excellent performance under normal operation and accident conditions. One of the design goals of modular HTGRs is to meet the U.S. Environmental Protection Agency's Protective Action Guides for offsite dose at the exclusion area boundary (EAB). To achieve this, the reactor design concepts require a level of fuel integrity that is far better than that achieved for all prior U.S. manufactured tristructural isotropic (TRISO) coated-particle fuel.

The overall goals of the Advanced Gas Reactor (AGR) Fuel Development and Qualification Program, as stated in the technical program plan [1], are to:

- Provide a baseline fuel qualification data set in support of the licensing and operation of the Generation IV very high temperature reactor (VHTR) (and a HTGR)
- Support near-term deployment of a VHTR (or HTGR) for commercial energy production in the U.S. by reducing market entry risks posed by technical uncertainties associated with fuel production and qualification
- Utilize international collaboration to extend the value of U.S. Department of Energy (DOE) resources.

The overarching objective of the AGR program is to qualify uranium oxycarbide (UCO)^a TRISO-coated particle fuel for use in a modular HTGR. TRISO-coated particles must be fabricated at engineering scale, as opposed to small batches in a laboratory, for use in qualification testing.^b The fuel development and qualification activities under the AGR Fuel program include fuel manufacturing process and quality control (QC) methods development, irradiation testing, post-irradiation examination (PIE), post-irradiation heating tests to simulate HTGR accident conditions, and fuel performance model development and validation. These activities are intended to first demonstrate that fuel fabricated to a particular set of fuel product and process specifications will meet the fuel performance requirements for the HTGR. The next step is to qualify fuel manufactured in production-scale equipment by irradiation testing and post-irradiation heating tests of statistically significant quantities of fuel. The final step is to establish limiting service conditions for the fuel. The testing, consisting of a variety of experiments and examinations, will enable an understanding of the behavior of TRISO-coated fuel under the radiation and temperature environments expected in an HTGR during normal operation and accident conditions. The

-
- a. Uranium oxycarbide as used here is a shorthand term to denote a mixture of uranium dioxide and uranium carbide, the two phases present in the kernel.
- b. In reading through AGR program information, the reader might see mention of UO₂ TRISO-coated particle fuel performance. Some limited work on UO₂ is being conducted in AGR-2 as part of an international collaboration under the auspices of the Generation IV International Forum, but the AGR program is predominantly focused on UCO TRISO-coated particle fuel and UO₂ will not be discussed in this report.

program includes experiments to provide an understanding of how the fission products are retained by or transported through the fuel particle kernel, particle coatings, and the carbonaceous matrix that compose the reactor core to support the reactor source term calculations. Another important part of the program is the development of fuel-performance and source-term modeling and simulation tools for use in the HTGR design, safety analyses, and licensing. Validation of fuel performance and fission product transport models with respect to their ability to accurately predict the performance of the fuel and the associated source term under both normal reactor operating conditions and accident conditions—which was part of the original program—is no longer part of the AGR program with the cessation of the Next Generation Nuclear Plant (NGNP) project.

At the start of the AGR program [2,3], without a reactor design concept selected from among modular HTGR alternatives, the program decided to qualify fuel to an operating envelope that would bound both pebble-bed and prismatic options. This resulted in needing a fuel form that could survive at peak fuel temperatures of 1,250°C on a time-averaged basis and high burnups in the range of 150 to 200 GWd/MTHM (metric tons of heavy metal) or 16.4 to 21.8% fissions per initial metal atom (FIMA). The program selected UCO as the fissile kernel of choice because of its ability to limit CO production and kernel migration under irradiation, phenomena that were considered potentially life limiting in the traditional UO₂ TRISO fuels operating at the upper temperature range (~1,250°C) and high burnup of a prismatic HTGR. Figure 1 is a radar plot of the five most important parameters for qualifying fuel performance: (1) fuel temperature, (2) fuel burnup, (3) fuel fast fluence, (4) power density, and (5) particle packing fraction. Envelopes are shown for the successful German and Japanese programs established in the 1980s and 1990s, respectively, along with a prismatic NGNP design. Because a final core design for the NGNP had not yet been established, a bounding envelope was established. The irradiations in the AGR program are using this envelope to guide the irradiation testing.

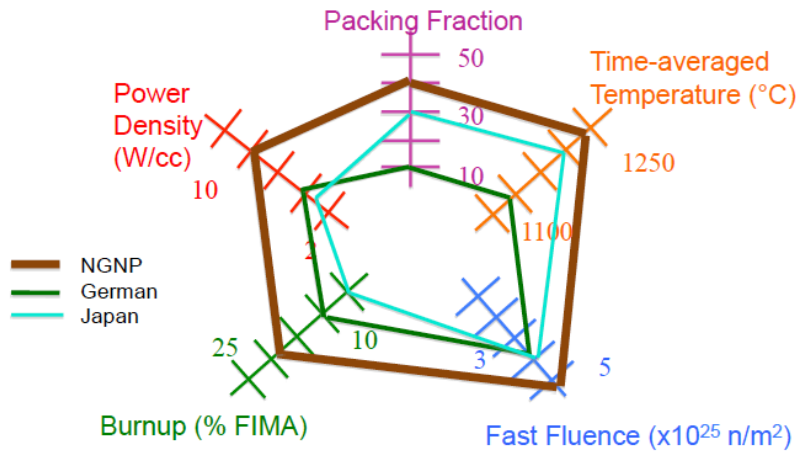


Figure 1. Radar plot of key parameters for TRISO-coated fuel performance.

2. FUNCTIONAL CONTAINMENT AND TRISO FUEL REQUIREMENTS

HTGRs have multiple barriers to radionuclide release that comprise a “functional containment.” The functional containment is the collection of design selections that, taken together, ensure that (a) radionuclides are retained within multiple barriers, with emphasis on retention at their source in the fuel, and (b) regulatory requirements and plant design goals for release of radionuclides are met at the EAB. In the U.S. the first three functional containment barriers consist of the fuel kernel, the fuel particle coatings, and the fuel matrix/graphite. The next barrier is the helium pressure boundary. The reactor building is the final barrier. The degree that each barrier is relied upon in a specific accident sequence is at the discretion of the designer. Tradeoffs can exist between the required effectiveness of the different barriers [4]. However, taken collectively, the barriers reduce releases of fission products to very low

levels during normal operation and postulated accident conditions [5]. Thus, there is a strong linkage between the behavior of TRISO fuel in a modular HTGR and the licensing strategy that is being employed in the U.S.

Successfully executing this strategy requires that (a) high-quality, low defect TRISO fuel can be fabricated and characterized in a repeatable and consistent manner, (b) fuel performance with very low in-service failures is achievable within anticipated modular HTGR fuel design envelope, and (c) a mechanistic source term can be calculated to the requisite level of accuracy for both normal and off-normal conditions. Modular HTGR designers have established fuel performance requirements that guide the fuel qualification and ensure that offsite dose design objectives will be met. Table 1 lists the level of allowable fuel defects and the allowable levels of in-service failures under normal operation and postulated core heatup accidents at 95% confidence based on the modular HTGR prismatic design and HTR MODUL pebble bed. They are very similar despite differences in design service conditions of the fuel (e.g., burnup, fast fluence, and temperature).

Table 1. Allowable fuel defect levels and in-service failures.

	Modular HTGR Prismatic	HTR MODUL Pebble
Manufacturing Defect Level		
Heavy metal contamination	2E-05	6E-05
Silicon carbide defects	1E-04	
In-Service Performance Requirements		
Incremental failures, normal operation	2E-04	1.6E-04
Incremental failures, core heatup accidents	6E-04	6.6E-04

3. FABRICATION

The TRISO-coated particle is a spherical-layered composite about 1 mm in diameter. It consists of a kernel of UO_2 or UCO surrounded by a porous carbon buffer layer that absorbs kinetic energy of fission fragments and allows space for fission gases to accumulate. Surrounding the buffer layer is a layer of dense pyrolytic carbon called the inner pyrolytic carbon layer (IPyC), a silicon carbide (SiC) layer, and a dense outer pyrolytic carbon layer (OPyC).

The uranium-containing kernels are made by a sol-gel process that is followed by washing, drying, calcining, and sintering to produce UCO kernels. UCO is a mixture of UO_2 , UC, and UC_2 and is formed by dispersing carbon in the sol-gel bead and performing a carbothermic reduction after calcination. The coatings are applied in a fluidized-bed coater in a sequential, continuous process. The coating process for the buffer is based on chemical vapor deposition from a mixture of acetylene and argon diluent. The inner and outer pyrolytic layers are deposited from a mixture of acetylene, propylene, and argon diluent. The SiC layer is deposited from methyltrichlorosilane (MTS) diluted with hydrogen and argon. Graphite powders and phenolic binder are used to produce a powder matrix that is applied to the TRISO particles as an overcoat. The overcoated particles are then pressed to form the pebble or cylindrical compact. Both fuel forms undergo carbonization and heat treatment at high temperature to produce the final fuel form. Rigorous control is applied at every step of the fabrication process to produce high-quality, very-low-defect fuel. Specifications are placed on the diameters, thicknesses, and densities of the kernel and coating layers; the sphericity of the kernel and coated particle; the stoichiometry of the kernel; the maximum anisotropy of the pyrocarbon layers; the microstructure of the SiC; and the acceptable defect levels for each layer. Statistical sampling techniques are used to demonstrate compliance with the

specifications, usually at the 95% confidence level [6]. The QC techniques used to meet each specification are shown in Table 2.

Table 2. QC methods for TRISO-coated particle fuel.

Property	QC Method
Kernels	
Uranium content	Wet chemistry
U-235 enrichment	Mass spectrometry
Impurities	Emission spectrometry, wet chemistry, and/or inductively coupled plasma mass spectrometry
C/U ratio	Combustion (carbon) and wet chemistry (uranium)
O/U ratio	Combustion (oxygen) and wet chemistry (uranium)
Bulk density	Mercury pycnometry
Diameter	Radiography, ceramography, optical shadow
Coatings	
Missing buffer fraction	Radiography (or sieving)
Buffer density	Calculated from particle density and volume (by mercury pycnometry)
Coating thicknesses	Radiography or ceramography
IPyC and OPyC anisotropy	Bacon Anisotropy Factor (BAF ₀) by reflection of polarized light
IPyC and OPyC density	Liquid density gradient column
SiC density	Liquid density gradient column
Defective IPyC coating fraction (fuel dispersion)	High-resolution X-ray radiography of loose particles previously heated to 1800°C for 1 hour.
OPyC surface connected porosity	Mercury porosimetry
SiC microstructure	Ceramography
Faceting	Radiography, ceramography, optical shadow
Missing or defective OPyC fraction	Optical microscopy
Gold spots (soot inclusions) in SiC coatings	Optical microscopy of loose and mounted particles
Compacts	
Uranium loading	Wet chemistry
Integrity and dimensions	Visual inspection and manual gauging
Matrix density	Calculation
Heavy metal contamination	Acid leach or gaseous HCl leach
Defective SiC coating fraction	Burn-leach
Defective OPyC coating fraction	Compact deconsolidation/optical microscopy
Impurities	Inductively coupled plasma mass spectrometry or glow discharge mass spectroscopy

Many improvements in the fabrication processes have been made in the AGR program. In the fabrication of kernels, internal gelation was used to improve sphericity, compared to external gelation, and the method of carbon addition was modified to improve distribution of oxide and carbide phases. Improvements were made in the chemical vapor deposition processes, including (a) argon dilution during SiC coating, (b) coater retort design to improve yields (>95%), (c) use of mass flow controllers to control gas flows during coating deposition of each coating layer, and (d) implementation of an improved MTS vaporizer (leveraging computer chip industry) to evaporate MTS and deposit the SiC layer. Human interactions in the process were also removed by (a) replacing tabling with three-dimensional (3D) sieving of coated particles; (b) replacing multi-step matrix production (resin solvation, matrix mixing, kneading, drying, and crushing) with dry mixing and jet milling of matrix; (c) replacing rotary overcoating using flammable solvents with an automated fluidized bed overcoater that produces highly spherical, uniformly overcoated particles using only water as the wetting agent; and (d) using automated die filling and programmed punch travel to form compacts. And finally, in the area of measurement science, computer measurements of thicknesses, greatly improved anisotropy measurements via ellipsometry, and improved density measurements using better density column materials, and a laser micrometer for compact diameter have improved precision in characterizing TRISO fuel.

The coating attribute specifications used by the AGR program evolved from that developed by General Atomics (GA) based on their historical experience at Fort St. Vrain, modified as necessary to ensure that high-level radionuclide release criteria could be met for their modular HTGR designs. During the AGR program, attempts have been made to examine the coating specification from a fuel performance perspective and to establish which of the coating attributes are most critical to in-reactor performance and the appropriate critical limits for those attributes to be used in the specification. Results of the analysis [7] suggest that only a few of the specifications have an impact on the anticipated fuel performance in an HTGR. Specifically, the analysis found:

- There was little change in the overall TRISO-coated particle failure probability as the attributes for pyrocarbon density (both IPyC and OPyC) and anisotropy were varied over the typical range of values. This is probably due to the uncertainties in the material properties, especially irradiation-induced creep.
- When varying the thickness of the SiC layer, the failure probability increased as the thickness decreased, because there is less structural material to retain the fission gas pressure and subsequent increase in tangential stress in the layer. Thus, a critical limit on the minimum thickness of SiC is warranted.
- Conversely, failure probability increased as the IPyC layer thickness increased, because more pyrocarbon causes an increase in shrinkage early in irradiation. This results in a higher IPyC cracking probability, causing localized stress concentrations in the SiC layer. Thus, a critical limit on the maximum IPyC thickness is warranted.
- As the buffer thickness decreases, the volume available to store fission gas decreases, resulting in a higher pressure and hence higher stress in the SiC layer. Thus, a critical limit on the minimum buffer thickness is warranted.
- For aspherical particles, as characterized by the aspect ratio (largest diameter divided by smallest diameter on a particle), the model used in the analysis treats asphericity essentially as a flat plate on one side of the particle. Increasing the aspect ratio increases the surface area of the flat plate, increasing the stress in the SiC layer due to pressure accumulation. Thus, a critical limit on aspect ratio is warranted.

These critical limits are in agreement with the specification. Similarly, process development was conducted to identify the critical process specifications necessary for fabrication of the PyC and SiC layers, which had historically been found to be the reason for poor U.S. fuel particle performance.

The overall evolution of fuel fabrication for each of the AGR experiments is shown in Table 3. Fabrication of the UCO fuel kernels has always been at engineering scale given the previous existing capabilities at BWX Technologies, Inc. (BWXT). Coatings and compacts began at laboratory scale. A 2-in. chemical vapor disposition coater at Oak Ridge National Laboratory (ORNL) was used with a 64-g uranium kernel charge to deposit coatings onto the UCO kernels used in AGR-1. A single compact press was used to produce the compacts for AGR-1. In AGR-2, both the kernels and coatings were produced at engineering scale while the compacting was still performed at laboratory scale at ORNL. A 6-in. chemical vapor disposition coater with a 1.3-kg charge of UCO kernels was used to deposit the coatings on kernels for use in AGR-2. Between AGR-2 and AGR-5/6/7, process development efforts focused on increasing the charge size in the coater for economic reasons and industrializing the compacting process. During AGR-5/6/7, the formal fuel qualification irradiation, the entire process was conducted at engineering scale. An automated overcoating and pressing process prototype was developed at BWXT to produce compacts at a rate of 3-4 compacts per minute for the first core of a 600-MWth HTGR. This capability established a full engineering pilot line at BWXT for TRISO-coated particle fuel. For actual production at full industrial scale, two options are available: (a) replication of the engineering pilot line to obtain the required capacity or (b) scale up of parts of the process for greater throughput and less replication. Option (a) was chosen for NGNP to meet the overall deployment schedule of the reactor. Three parallel lines were estimated to meet throughput requirements for the fuel fabrication facility. Option (b) is a possible approach but entails potential requalification of the changes in the production process through additional process development and most likely an additional irradiation to provide the level of assurance anticipated from the regulatory authority. It is also anticipated that the entire design of the fuel fabrication facility would consider the potential for automation where possible to optimize production and minimize cost in an industrial setting. However, it is not anticipated that such automation improvements would influence the fundamental unit operations associated with TRISO-particle fuel fabrication and instead would improve efficiency in handling of kernels, particles, and compacts between the major unit operations. Much of the work on automation and preparing for fabrication of the first core of NGNP was curtailed when the NGNP program was terminated.

Table 3. Evolution of fuel fabrication in AGR program.

Experiment	Kernels	Coatings	Compacts
AGR-1	Engineering scale	Laboratory scale	Laboratory scale
AGR-2	Engineering scale	Engineering scale	Laboratory scale
AGR-5/6/7	Engineering scale	Engineering scale	Engineering scale

Table 4, Table 5, and Table 6 provide typical attributes of UCO and UO₂ kernels, TRISO-coated particles, and fuel compacts used for the AGR-2 irradiation.

Table 4. UCO and UO₂ kernel attributes for use in AGR-2 irradiation.

Property	Specified Range for Mean Value	Actual Mean Value ± Population Standard Deviation
UCO^a		
Diameter (μm)	425 ± 20	426.7 ± 8.8
Density (Mg/m ³)	≥10.4	10.966 ± 0.033
U-235 enrichment (wt%)	14.0 ± 0.10	14.029 ± 0.026
Carbon/uranium (atomic ratio)	0.40 ± 0.10	0.392 ± 0.002
Oxygen/uranium (atomic ratio)	1.50 ± 0.20	1.428 ± 0.005
[Carbon + oxygen]/uranium (atomic ratio)	≤2.0	1.818 ± 0.005
Total uranium (wt%)	≥88.5	89.463 ± 0.051
Sulfur impurity (ppm – wt)	≤1,500	365 ± 12
Phosphorus impurity(ppm – wt)	≤1,500	≤30
All other impurities (ppm – wt)	≤100	Below minimum detection limits and within specification
UO₂^b		
Diameter (μm)	500 ± 20	507.7 ± 11.9
Density (Mg/m ³)	≥10.3	10.858 ± 0.082
U-235 enrichment (wt%)	9.6 ± 0.10	9.600 ± 0.010
Oxygen/uranium (atomic ratio)	1.98 ≤ O/U ≤ 2.01	2.003 ± 0.005
Phosphorus, sulfur impurities (ppm – wt)	≤1,500	≤30 for phosphorus; ≤25 for sulfur
All other impurities (ppm-wt)	≤100	Below minimum detection limits and within specification
a. BWXT UCO kernel lot G73I-14-69307		
b. BWXT UO ₂ kernel lot G73AA-10-69308		

Table 5. Properties of TRISO-coated UCO and UO₂ particles for use in AGR-2 irradiation.

Property	Specified Range for Mean Value	Actual Mean Value ± Population Standard Deviation	
		UCO	UO ₂
Buffer thickness (μm)	100 ± 15	98.9 ± 8.4	97.7 ± 9.9
IPyC thickness (μm)	40 ± 4	40.4 ± 2.5	41.9 ± 3.2
SiC thickness (μm)	35 ± 3	35.2 ± 1.2	37.5 ± 1.2
OPyC thickness (μm)	40 ± 4	43.4 ± 2.9 ^a	45.6 ± 2.4 ^a
Buffer density (Mg/m ³)	1.05 ± 0.10	Not measured ^{b,d}	0.99 ^c
IPyC density (Mg/m ³)	1.90 ± 0.05	1.890 ± 0.011	Not measured ^{b,d}
SiC density (Mg/m ³)	≥3.19	3.197 ± 0.004	3.199 ^e
OPyC density (Mg/m ³)	1.90 ± 0.05	1.907 ± 0.007	1.884 ± 0.004
IPyC anisotropy (BAF _o) ^h	≤1.045	1.0349 ± 0.0012	1.0334 ± 0.0027
OPyC anisotropy (BAF _o) ^h	≤1.035	1.0263 ± 0.0011	1.0219 ± 0.0012
IPyC anisotropy post compact anneal (BAF _o) ^h	Not specified	1.0465 ± 0.0049	1.0471 ± 0.0036
OPyC anisotropy post compact anneal (BAF _o) ^h	Not specified	1.0429 ± 0.0019	1.0365 ± 0.0016
SiC sphericity (aspect ratio)	Mean not specified ^f	1.037 ± 0.011	1.034 ± 0.010
OPyC sphericity (aspect ratio)	Not specified	1.052	1.052
Particle diameter ^g (μm)	Mean not specified	873.2 ± 23	953.0 ± 28
Particle mass (mg)	Mean not specified	1.032 ± 0.003	1.462 ± 0.005

a. Ninety-five percent upper confidence thickness exceeds specifications. Justification of acceptance: OPyC thickness does not affect the compacting process or the fuel performance during irradiation

b. BWXT's hot sampling system did not allow both buffer and IPyC density measurements.

c. Single determination; no statistical confidence available.

d. Similar samples showed measurement results within specifications

e. Lower confidence level.

f. Critical region is specified such that ≤1% of the particles shall have an aspect ratio ≥1.14 for UCO fuel and ≥1.10 for UO₂ fuel.

g. Based on mean average particle measurements, not sums of mean layer thicknesses.

h. BAF_o equivalent calculated using diattenuation (N) and the equation $BAF_o = 1+3 \cdot N$.

Table 6. Selected properties for AGR-2 compacts.

Property	Specified Range for Mean Value	Actual Mean Value ± Population Standard Deviation	
		UCO	UO ₂
Compact mass (g)	Not specified	6.294 ± 0.011	6.103 ± 0.015
Mean uranium loading (g U/compact)	1.265 ± 0.07 (UCO) 1.00 ± 0.05 (UO ₂)	1.257 ± 0.03	0.993 ± 0.006
Diameter ^a (mm)	12.22 – 12.46	12.286 ± 0.005	12.269 ± 0.007
Length ^a (mm)	25.02 – 25.40	25.141 ± 0.017	25.135 ± 0.018
Number of particles per compact ^b	Not specified	3,176	1,543
Particle volume packing fraction (%)	Not specified	37	23
Effective overall compact density ^b (Mg/m ³)	Not specified	2.11	2.05
Compact matrix density (Mg/m ³)	≥1.45	1.589 ± 0.005	1.680 ± 0.008
Compact weight % U ^b	Not specified	19.97	16.27
Compact weight % O ^b	Not specified	1.92	2.19
Compact weight % Si ^b	Not specified	6.85	4.54
Compact weight % C ^b	Not specified	71.26	77.00
Iron content (µg Fe outside of SiC/compact)	≤25	4.04	2.75
Chromium content (µg Cr outside of SiC/compact)	≤50	0.61	0.48
Manganese content (µg Mn outside of SiC/compact)	≤50	0.136	0.133
Cobalt content (µg Co outside of SiC/compact)	≤50	0.115	0.113
Nickel content (µg Ni outside of SiC/compact)	≤50	0.96	0.59
Calcium content (µg Ca outside of SiC/compact)	≤50	39.34	35.16
Aluminum content (µg Al outside of SiC/compact)	≤50	29.60	42.69
Titanium content (µg Ti outside of SiC/compact)	Footnote c	2.81	3.31
Vanadium content (µg V outside of SiC/compact)	Footnote c	17.09	15.41
U contamination fraction ^d (g exposed U / g U in compact)	≤ 2.0×10 ⁻⁵	≤ 2.5×10 ⁻⁵ (e)	≤ 3.2×10 ⁻⁵ (e)
U contamination fraction w/o exposed kernels (g leached U / g U in compact)	Not specified	1.59×10 ⁻⁶	1.57×10 ⁻⁶
Defective SiC coating fraction ^d	≤ 1.0×10 ⁻⁴	≤ 1.2×10 ⁻⁵	≤ 2.5×10 ⁻⁵
Defective IPyC coating fraction ^d	≤ 1.0×10 ⁻⁴	≤ 4.8×10 ⁻⁵	≤ 7.7×10 ⁻⁵
Defective OPyC coating fraction ^d	≤ 1.0×10 ⁻²	≤ 9.5×10 ⁻⁴	≤ 2.0×10 ⁻³
<p>a. Allowable range corresponding to upper and lower critical limits specified with no compacts exceeding the limits, which require 100% inspection of all compacts.</p> <p>b. Approximate calculated value derived from other characterized properties.</p> <p>c. Mean value specification of ≤ 240 µg Ti plus V outside SiC/compact.</p> <p>d. Value is an estimate of an attribute property, not the mean of a variable property.</p> <p>e. Values represent 95% confidence levels and exceed specification.</p>			

The overall result from the AGR fuel fabrication efforts has been controllable and reproducible fabrication and improved characterization of the fuel forms, all of which contribute to better quality TRISO fuel [8, 9, 10]. Figure 2 compares the standard deviation in coating layer thicknesses from historical German, Japanese, and U.S. fuel with recent results from the AGR program. In almost all cases, the standard deviation of the coating layers is as good as, or slightly better than, the historical data.

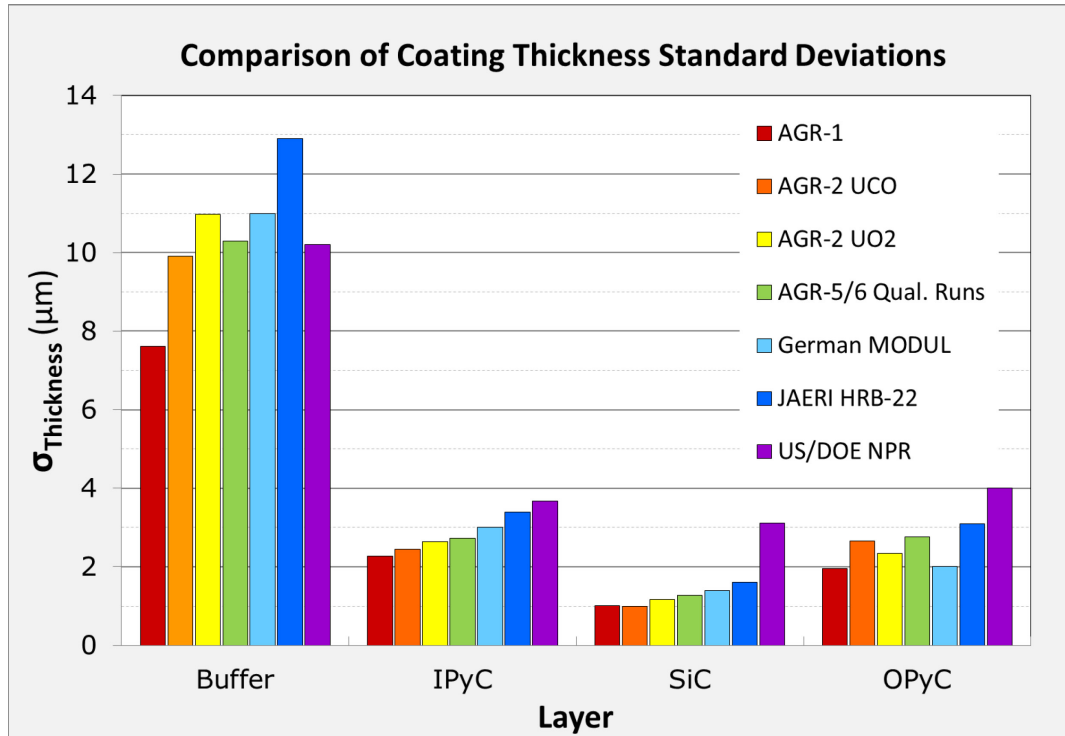


Figure 2. Comparison of standard deviation of coating layer thicknesses from the AGR program with historic German, Japanese, and U.S. TRISO fuel.

A comparison of a few of the key types of defects at laboratory scale for AGR-1 and at engineering scale for AGR-2 TRISO fuel is shown in Table 7. As might be anticipated, the defect level at the engineering scale is somewhat greater than at laboratory scale. (The specification level was not as stringent for AGR-1 as for AGR-2, so samples sizes were smaller.)

Recent work in which five coating runs were performed at the same conditions indicate a high degree of repeatability [11]. Despite the stochastic nature of the chemical vapor deposition process, physical fuel attributes such as layer thicknesses, layer densities, and layer anisotropy show very little variation from batch to batch.

Figure 3 compares the defect levels for coating results for AGR-2 and other developmental coating runs to previous German data, all at 95% confidence. Heavy metal contamination in most cases is below $5E-05$, with a few of the more recent coating runs closer to the specification value of $2E-05$. SiC defects are generally well below the $1E-04$ specification. In terms of total leachable uranium, the results in most cases are comparable to German results, with most data meeting the pebble-bed specification of $6E-05$. Thus, it is concluded that AGR fuel meets physical specifications and is meeting almost all defect specifications at 95% confidence. With larger sample sizes and a mature process, the fuel should be able to meet the defect specifications in production mode.

In summary, systematic fabrication studies, combined with improved characterization capabilities, have also enhanced the understanding of how to fabricate high-quality TRISO fuel. The program is now

using an engineering-scale coater to fabricate high-quality, TRISO-coated fuel particles that exhibit a rate of less than five defects in every 100,000 particles at 95% confidence due to flawed coatings (SiC or IPyC) or exposed uranium. Placing a U.S. fuel vendor in position to fabricate high-quality TRISO fuel with an improved fundamental understanding of the relationships among the fuel fabrication process, fuel properties, and fuel performance enhances credibility in establishing the safety case and the licensing basis. Today, the U.S. fuel vendor (BWX Technologies Nuclear Operations Group-Lynchburg [BWXT]) has all of the technologies necessary to fabricate TRISO-coated UO₂ or UCO fuel in compact form. A pilot line has been established, and fuel fabrication for final fuel qualification testing has begun.

Table 7. Comparison of defects at laboratory (AGR-1) and engineering (AGR-2) scale. Fractional defect values are 95% confidence estimates based on sample size. The AGR-1 data are reported for each different fuel type: Baseline, Variant 1, Variant 2, and Variant 3 (B, V1, V2, and V3, respectively).

	AGR-1 B	AGR-1 V1	AGR-1 V2	AGR-1 V3	AGR-2 UCO	AGR-2 UO ₂
At Particle Level						
SiC defects	0/120,688 ≤2.5E-5	1/121,117 ≤4.0E-5	1/50,265 ≤9.5E-5	1/120,660 ≤4.0E-5	5/217,000 ≤4.9E-5	1/120,000 ≤4.0E-5
Compact Level						
Exposed U defects	0/99,470 ≤3.1E-5	0/74,699 ≤4.1E-5	0/99,100 ≤3.1E-5	0/99,032 ≤3.1E-5	3/317,625 ≤2.5E-5	3/246,840 ≤3.2E-5
IPyC defects	0/49,735 ≤6.1E-5	0/49,799 ≤6.1E-5	0/49,555 ≤6.1E-5	0/49,516 ≤6.1E-5	0/63,525 ≤4.8E-5	1/61,710 ≤7.7E-5
SiC defects	2/49,735 ≤1.3E-4	0/49,799 ≤6.1E-5	1/49,555 ≤9.6E-5	0/49,516 ≤6.1E-5	0/254,100 ≤1.2E-5	0/123,420 ≤2.5E-5

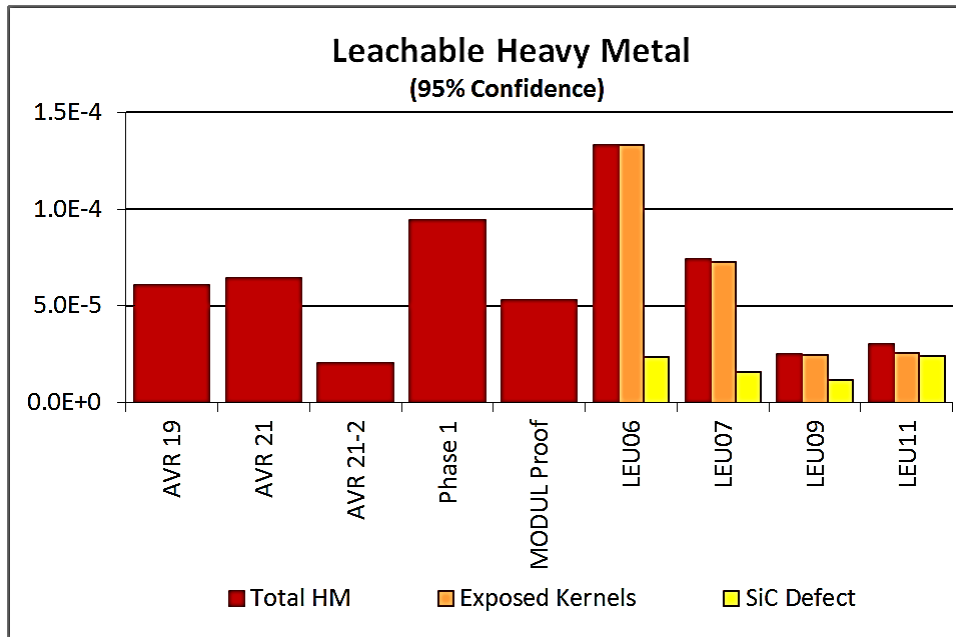


Figure 3. Comparison of heavy metal contamination, SiC defect fraction, and total leachable heavy metal for AGR-2 and development coating runs compared to historic German fuel.

4. IRRADIATION PERFORMANCE

The objective of AGR fuel irradiation activities is to provide data on TRISO-coated UCO fuel performance under normal operation to initially demonstrate and then qualify fuel for operation in an HTGR. The objectives of these tests are to provide irradiation performance data to support fuel process development, qualify fuel for normal operating conditions and accident conditions, and support development and validation of fuel performance and fission product transport models. A further underlying objective of the AGR Fuel Program is to further the development of a fundamental understanding of the relationships among the fuel fabrication process, fuel product properties, and irradiation and accident condition performance, which will lead to improved models for predicting the performance of the fuel. Table 8 summarizes the planned irradiation testing program.

Table 8. AGR fuel program irradiation tests.

Capsule	Test Description	Test Objective/Expected Results
AGR-1	<p>Shakedown Test/Early Fuel Performance Demonstration Test</p> <p>Contents included compacts made from UCO fuel particles coated in a 2-in. laboratory-scale coater at ORNL. A baseline fuel particle composite and three variant fuel particle composites were tested. The variants included two particle composites coated using different IPyC coating conditions and one particle composite coated using different SiC coating conditions.</p>	<p>Gain experience with multi-cell capsule design, fabrication, and operation to reduce chances of capsule or cell failures in subsequent capsules. Obtain early data on irradiated fuel performance, and support development of a fundamental understanding of the relationship among fuel fabrication process, fuel product properties, and irradiation performance. Provide irradiated UCO fuel for accident simulation testing (i.e., heating tests).</p>

Table 8. (continued).

Capsule	Test Description	Test Objective/Expected Results
AGR-2	<p>Fuel Performance Demonstration Fuel Contents included compacts containing UCO particles made in a large coater and UO₂ particles made by BWXT, AREVA/CEA, and Pebble Bed Modular Reactor in different size coat-ers. AGR-2 had six independently monitored and controlled capsules in a test train design that was essentially the same as that demonstrated in AGR-1. One capsule of UCO fuel was operated with a maximum time-averaged temperature of about 1,400°C as a performance margin test of the fuel.</p>	<p>Provide irradiation performance data for UCO and UO₂ fuel variants and irradiated fuel samples for PIE and post-irradiation heating tests to broaden options and increase prospects for meeting fuel performance requirements and to support development of a fundamental understanding of the relationship among the fuel fabrication process, fuel product properties, and irradiation performance. Also, establish the irradiation performance margin for UCO fuel.</p>
AGR-3/4 ^a	<p>Fission Product Transport Contents included compacts of low-enriched uranium (LEU) UCO particles seeded with designed-to-fail LEU UCO particles to provide a well-defined fission product source. The fuel test element utilized a concentric-ring design to provide a one-dimensional geometry to facilitate derivation of effective diffusivities. Test capsules operated at different temperatures, and operation was maintained isothermal to the extent practical.</p>	<p>Provide data on fission gas release from failed particles, fission metal diffusion in kernels, and gas and metal diffusion in coatings for use in development of fission product transport models.</p>
AGR-5/6 ^b	<p>Fuel Qualification Contents are to include a single fuel type made using process conditions and product parameters considered to provide the best prospects for successful performance based on process development results and available data from AGR-1 and AGR-2; variations in cell irradiation temperatures per test specification.</p>	<p>Provide irradiation performance data for the reference fuel and irradiated fuel samples for PIE and post-irradiation heating tests in sufficient quantity to demonstrate compliance with statistical performance requirements under normal operation and accident conditions.</p>
AGR-7	<p>Fuel Performance Margin Test Contents are to include the same fuel type as that used in AGR-5/6 but would be tested under service conditions that exceed the anticipated operating envelop in anticipation that some measurable level of fuel failure would occur (i.e., margin test).</p>	<p>Provide fuel performance data and irradiated fuel samples for PIE and post-irradiation heating tests and PIE in sufficient quantity to demonstrate the capability of fuel to withstand conditions beyond AGR-5 and -6 in support of plant design and licensing.</p>
<p>a. AGR-3 and -4 were originally planned with each test rig containing six independent capsules. The AGR program combined them into a single test, currently referred to as AGR-3/4, which is a test rig containing 12 independent capsules.</p> <p>b. AGR-5 and -6 were also originally planned as two separate irradiation tests, but they are now combined into a single test train along with AGR-7.</p>		

4.1 AGR-1 and AGR-2

The experiment test train for AGR-1 consisted of six separate stacked capsules vertically centered in the core of the Advanced Test Reactor (ATR) at Idaho National Laboratory. Each capsule had its own custom blended gas supply and exhaust for independent temperature control and fission product monitoring. Temperature control of the capsules was accomplished by adjusting the mixture ratio of two gases with differing thermal conductivities to control the heat transfer across an insulating gas jacket between the heat source (fuel fissions and gamma heating of capsule materials) and the relatively cold

reactor coolant (52°C). Helium was used as the high (thermally) conductive gas, and neon was used as the insulating gas.

A horizontal capsule cross section at the top of the AGR-1 test train is shown in Figure 4. The capsules were approximately 35 mm (1-3/8 in.) in diameter and 150 mm (6 in.) in height, including the plenums between adjacent capsules. Each capsule contained 12 prototypical right circular cylinder fuel compacts nominally 12.3 mm (1/2 in.) in diameter and 25 mm (1.0 in.) long. For AGR-1, the fuel contained TRISO-coated, 350- μm UCO particles with a packing fraction of 37% and an enrichment of 19.74% U-235. For AGR-2, two different fuels were tested. The first fuel was TRISO-coated, 425- μm UCO particles with a packing fraction of \sim 37% and an enrichment of 14.0% U-235. The second fuel was TRISO-coated, 500- μm UO_2 particles with a packing fraction of \sim 23% and an enrichment of 9.6% U-235 (to allow sufficient heat in the test to attain temperature).^c

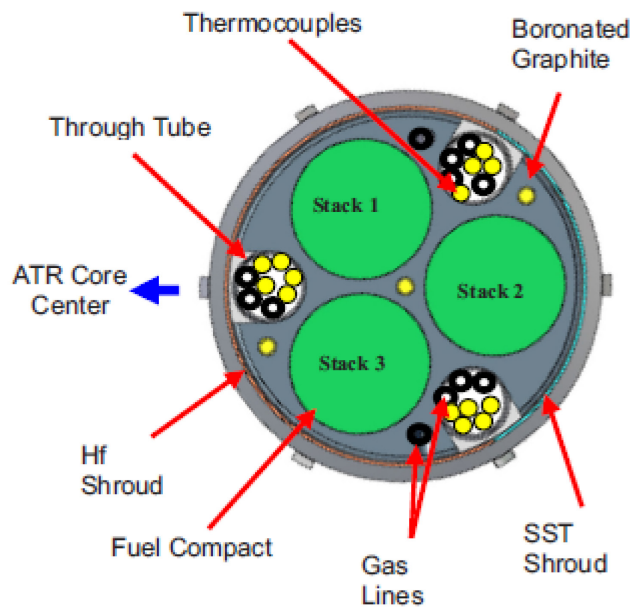


Figure 4. Horizontal cross section of an AGR-1 experiment capsule.

The experiment contained fuel compacts arranged in four layers in each capsule with three compacts per layer nested in a triad configuration. A nuclear-grade graphite spacer surrounded and separated the three fuel compact stacks in each capsule to prevent any fuel particles on adjacent compacts from touching each other, which could possibly cause a premature particle failure. The experiments contained (a) a number of thermocouples to measure temperature, (b) gas lines to route the effluent by gamma spectrometers to monitor for fission gas release and fuel failure, and (c) flux wires that were extracted during PIE to establish thermal and fast fluences in the experiments. Figure 5 shows a cross section of the ATR and the east large B position that was used for AGR-1. AGR-2 was similar in design but was a mirror image of AGR-1, since it was irradiated in an identical position on the other side of the ATR in the west large B position.

c. The particles fabricated for AGR-1 were based on the fissile particle in a two-particle fissile/fertile design by GA. Subsequently, the program moved to a single-particle design and developed the 425- μm /14 % enriched particle. For AGR-5/6/7, the same particle size will be used, but the enrichment increased slightly to 15.5% based on design studies conducted at GA prior to termination of the NGNP program.

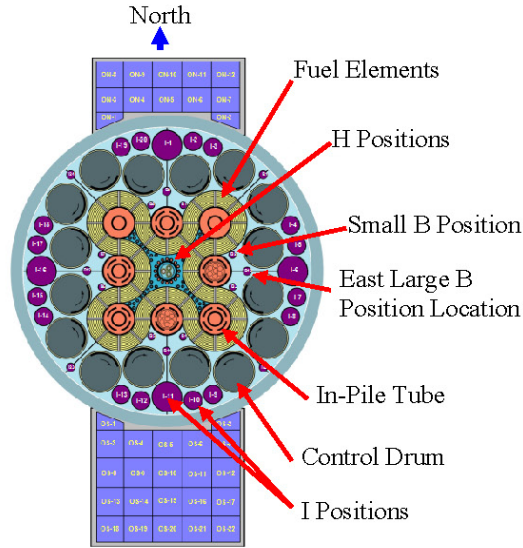


Figure 5. ATR core cross section.

To monitor fission gases, the system routed the outlet gas from each capsule to individual fission product monitors, as shown in Figure 6. The fission product monitors consisted of a spectrometer for identifying specific fission gases and a gross gamma detector to indicate when a puff release of fission gases passed through the monitor.

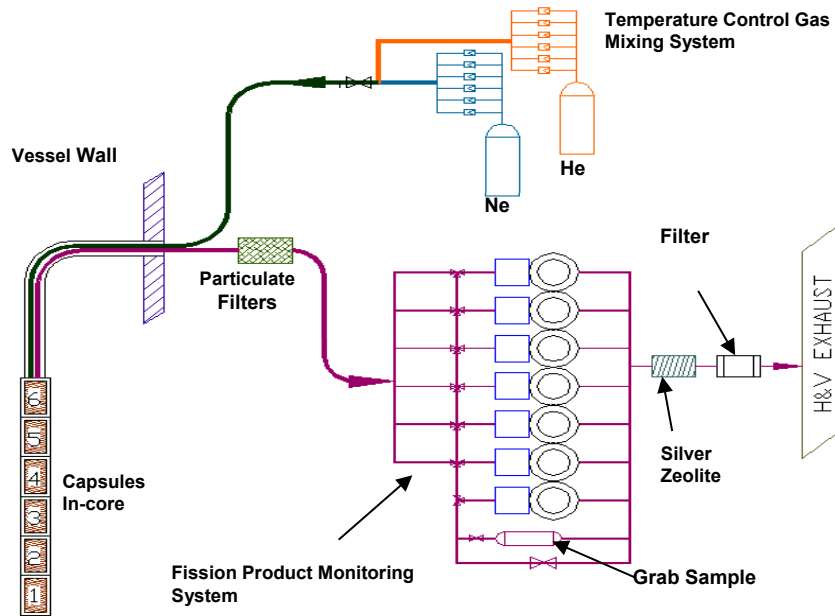


Figure 6. AGR-1 experiment flow path.

AGR-1 ended in 2009 after approximately 3 years of irradiation. The UCO fuel in AGR-1 was irradiated to a peak burnup of 19.6% FIMA, a peak fast-neutron fluence of about 4.3×10^{25} n/m², and a maximum time-averaged fuel temperature of <1,200°C. About 300,000 TRISO fuel particles were irradiated without a single particle failure, as indicated by the fission-gas measurements on the purge gas from each of the capsules [12].

The second irradiation, AGR-2, was a performance demonstration irradiation of fuel using a pilot-scale coater. It contained separate capsules to test UCO and UO_2 TRISO fuel produced at industrial scale from U.S. and international collaborators (France/AREVA/CEA and South Africa/ Pebble Bed Modular Reactor). The UCO was irradiated under prototypical prismatic core conditions, and the UO_2 TRISO temperature experienced conditions typical of a pebble-bed HTGR. The UCO fuel in the U.S. AGR-2 capsules was irradiated to a peak burnup of 13.2% FIMA, a peak fast-neutron fluence of about 3.5×10^{25} n/m^2 , and a maximum time-averaged fuel temperature of $<1,350^\circ\text{C}$. The UO_2 fuel in the U.S. AGR-2 capsule was irradiated to a peak burnup of 10.7% FIMA, a peak fast-neutron fluence of about 3.5×10^{25} n/m^2 , and a maximum time-averaged fuel temperature of $<1,100^\circ\text{C}$.

Fission gas release measured from both the AGR-1 and AGR-2 experiments is compared to historic German and U.S. irradiations in Figure 7. The gas release for AGR-1 was extremely low, indicating no particle failures during the irradiation. Thus, AGR-1 is the best irradiation performance of a large quantity of TRISO fuel ever achieved in the U.S., and the experiments substantially exceeded the German levels of burnup. These results have confirmed the expected superior irradiation performance of UCO at high burnup in that no kernel migration, no evidence of CO attack of SiC, and no indication of severe SiC attack by noble metal or lanthanide fission products has been observed. Zero fuel failures in AGR-1 translates into a 95% confidence failure fraction of $<1\text{E}-5$, a factor of 20 better than the prismatic reactor design in-service failure fraction requirement of $2\text{E}-4$.

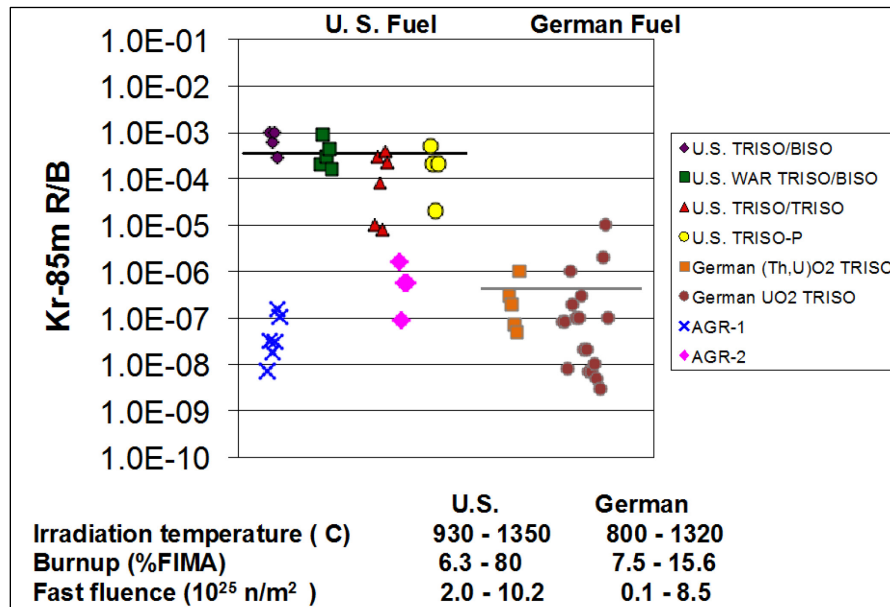


Figure 7. End-of-life Kr-85m fission gas release for AGR-1 and AGR-2 compared to historic performance in U.S. and German TRISO fuel irradiations

The in-pile results for AGR-2 shown in Figure 7 [13] are higher than AGR-1 and indicate one exposed kernel in each capsule based on the level of heavy-metal contamination measured during QC of the fuel. Detailed analysis of the three UCO test capsules [14] and current PIE results suggest that either zero particles or one particle may have failed in one UCO capsule based on fission gas release. Because of gas flow problems in the irradiation capsule that occurred about one-third of the way into the experiment, it is difficult to determine precisely. Thus, assuming zero or one particle failure out of 114,000 UCO TRISO particles, a 95% confidence failure fraction between $2.7\text{E}-05$ and $4.2\text{E}-05$ is obtained, which is a factor of about 5 to 7 below the designer specification of $2\text{E}-04$.

As indicated in Figure 8, the AGR-1 irradiation resulted in UCO TRISO fuel being exposed to very high temperatures for long times, well in excess of those expected in an actual modular HTGR. By comparison, peak time average temperatures in prismatic modular HTGRs are usually less than $1,250^\circ\text{C}$.

Based on the figure, about 15% of the particle population underwent temperatures in excess of 1,250°C for 200 days, 10% of particle population underwent temperatures in excess of 1,300°C for 100 days, 5% of particle population underwent temperatures in excess of 1,350°C for 50 days, and 2% of particle population underwent temperatures in excess of 1,400°C for 25 days. The more severe AGR-1 irradiation conditions, compared to the vast majority of historic modular HTGR designs, suggest a substantial fuel performance margin. Similar plots are provided in Figure 9 and Figure 10 for AGR-2, where the results from Capsule 2 are separated from Capsules 5 and 6, because it was designed to operate at a time-averaged peak temperature of 1,400°C (an early margin test), whereas the other two capsules were operated at a time-averaged peak temperature of $\leq 1,250^\circ\text{C}$.

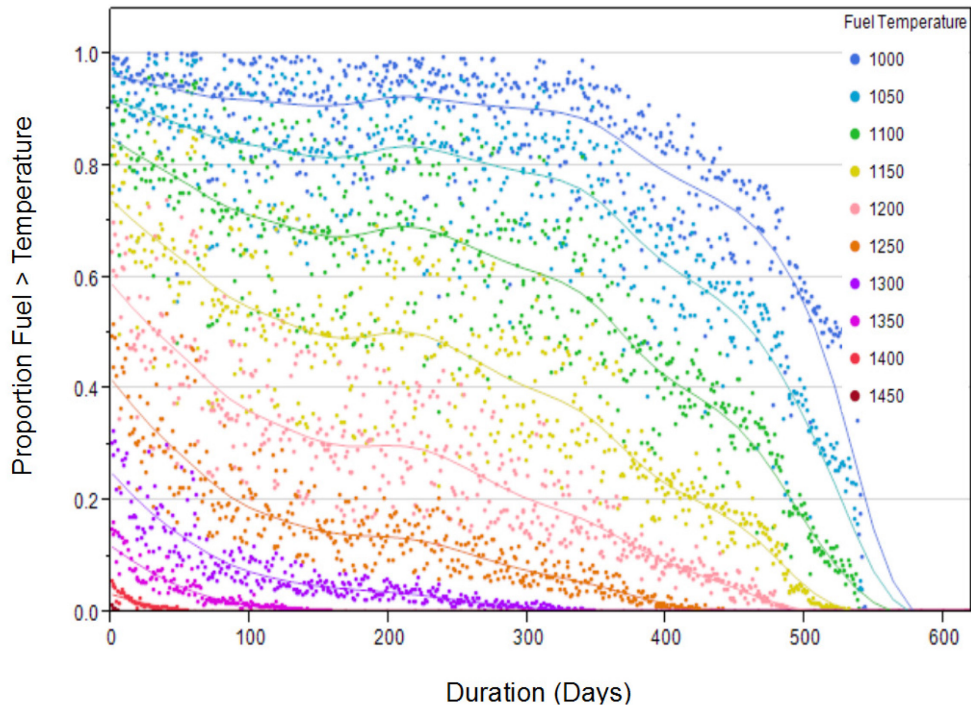


Figure 8. Distribution of time at temperature experienced by TRISO fuel particles in AGR-1.

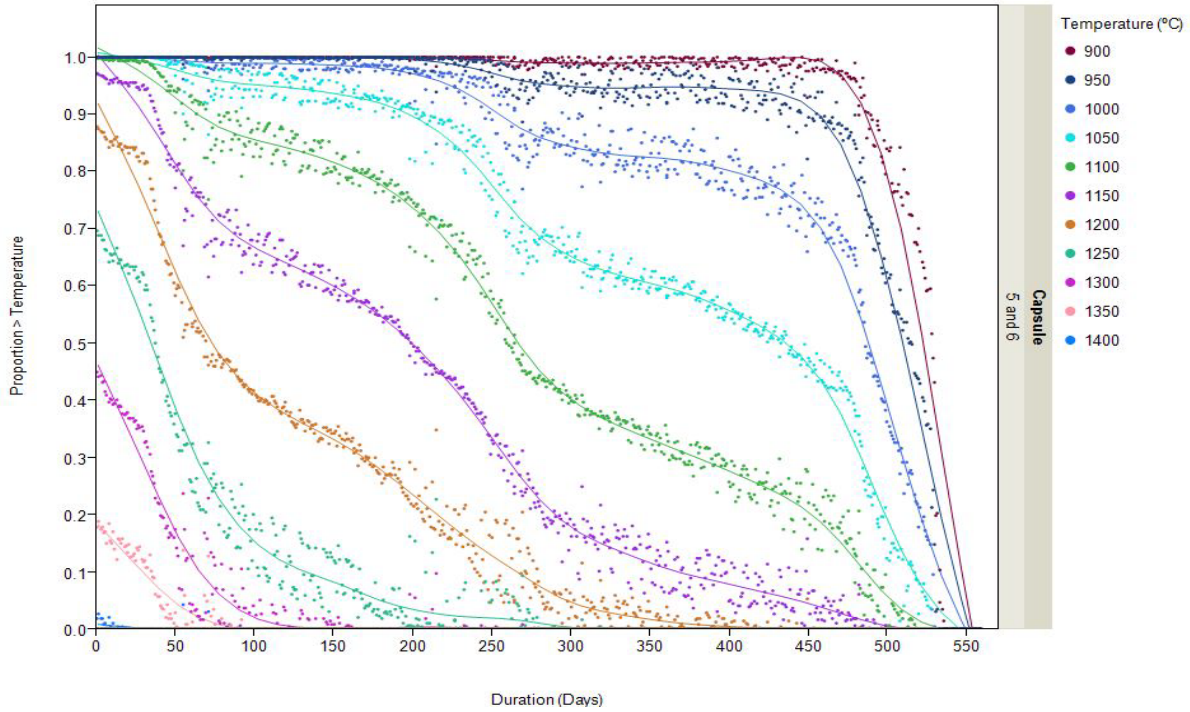


Figure 9. AGR-2 time at temperature for Capsules 5 and 6 (UCO fuel) (designed to operate at a time-averaged temperature of 1,250°C).

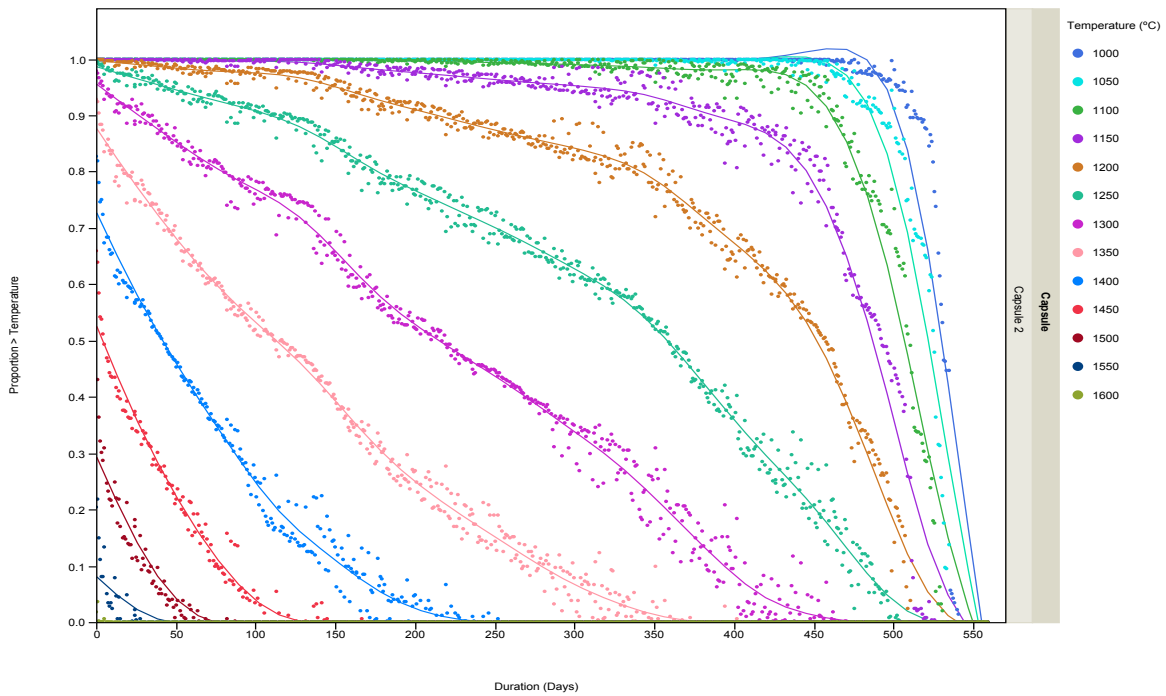


Figure 10. AGR-2 time at temperature for Capsule 2 (UCO fuel) (designed to operate at a time-averaged peak temperature of 1,400°C).

The calculated temperatures in AGR-2 are similar to those in AGR-1 in that much of the fuel operated at high temperature for significant amounts of time. A key result for AGR-2 is the results of Capsule 2 in

which large fractions of the fuel operated at very high temperature, i.e., in excess of 1,400°C, and up to 10% of the fuel underwent operation at 1,500°C for 30 to 50 days.

To provide another perspective of the severity of the AGR irradiations, the temperature distributions from the six capsules in AGR-1 and in Capsules 2, 5, and 6 of AGR-2 are compared to the distribution calculated for the steam cycle modular helium reactor (SC-MHR), a GA design with an outlet temperature of 750°C. As can be seen in Figure 11, the irradiations are very bounding in terms of temperature relative to that expected in the GA design. The effect would be even more exacerbated in the Xe-100 design, because pebble-bed reactors tend to run cooler than prismatic reactors at the same outlet temperature. The AGR program recognizes that the temperatures in the AGR-1 and AGR-2 irradiations are overly conservative relative to that expected in the reactor. Thus, for the final fuel qualification irradiation, the AGR program is taking efforts to develop a capsule design for AGR-5/6/7 that would produce temperatures that more closely mimic the distribution in a reactor while still being somewhat conservative. Additional details are found in the final as-run reports for the two irradiations [15,16].

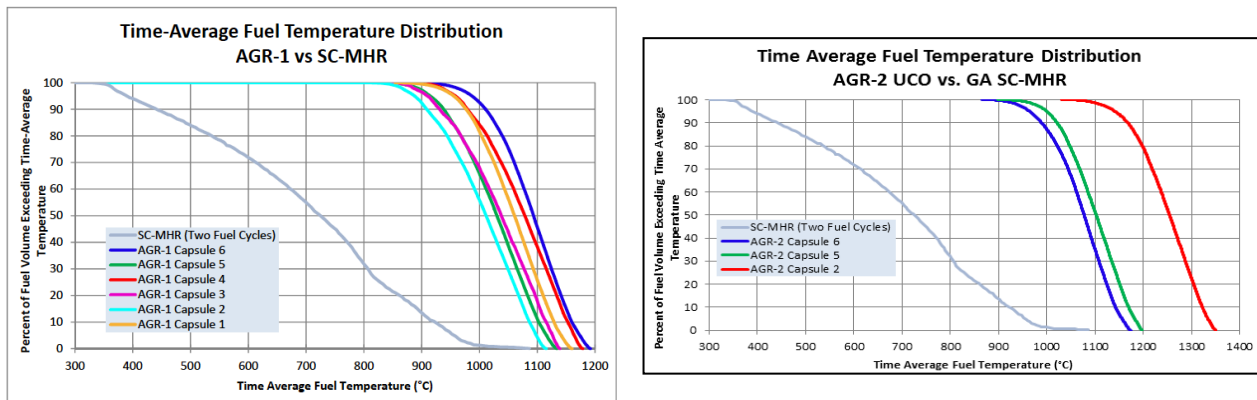


Figure 11. Comparison of fuel temperature distribution in AGR-1 and AGR-2 capsules with that expected from a 750°C outlet temperature HTGR (the General Atomics steam cycle modular helium reactor)

4.2 AGR-3/4

AGR-3/4 was the third and fourth in this series of planned experiments to test TRISO-coated UCO fuel. These were combined into a single experiment to reduce costs and overall program schedule. Details are found in Reference [17]. The objective of this experiment is very different than the objectives of AGR-1 or AGR-2. AGR-3/4 is devoted to understanding fission product transport behavior in TRISO particles and the graphitic components (fuel matrix and fuel element graphite) anticipated in an HTGR core. Thus, this experiment supports the HTGR source term evaluation and not TRISO-coated particle fuel performance assessment. The fuel irradiated in each AGR-3/4 capsule contained conventional TRISO driver fuel particles and designed-to-fail (DTF) fuel particles. The UCO kernels of conventional fuel particles were similar to the baseline fuel used in the AGR-1 experiment. The DTF fuel particles contained kernels identical to the driver fuel kernels, but the coatings on the DTF fuel particles were designed-to-fail under irradiation, leaving fission products to migrate through the surrounding materials. The same number of DTF fuel particles were embedded along the vertical centerline in each compact to offer a controlled geometry for the release from the DTF.

AGR-3/4, the most complex irradiation experiment performed in the AGR series, was composed of 12 independently controlled and monitored capsules stacked on top of each other to form the test train using the full 1.22-m active core height, as shown in Figure 12. Each capsule contained four 3.81-cm-long compacts. Each fuel compact contained about 1,872 conventional UCO driver-fuel-coated particles and 20 DTF UCO fuel particles. A leadout tube held the experiment in position and contained and protected the gas lines and thermocouple (TC) wiring extending from the test train to the reactor penetration. Three

TCs were located in Capsules 5, 10, and 12, and two TCs were used in each of the remaining capsules. The capsules were designed to span a range of temperatures, burnups, and fluences to establish correlations of fission product transport behavior with those service conditions.

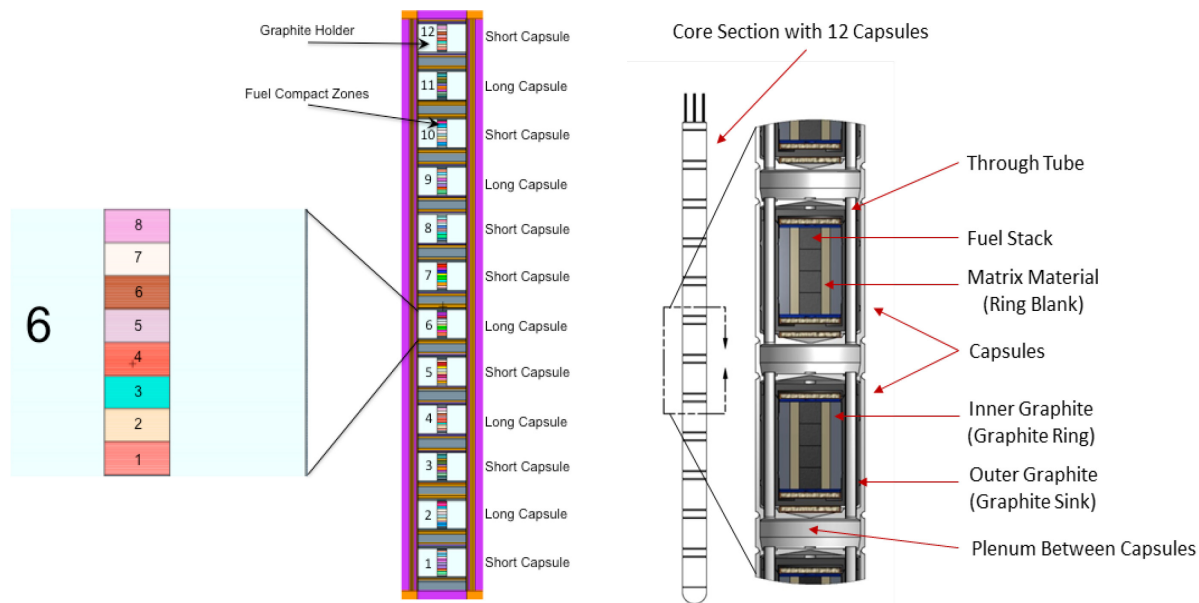


Figure 12. Axial (left) cross-section view and schematic (right) of AGR-3/4 capsules.

The irradiation was successfully completed in April 2014 after a total of 369.1 effective full power days. This ATR position allowed the program to achieve significant end-of-irradiation conditions in terms of peak burnup (15.3% FIMA) and maximum fast neutron fluence accumulation (5.3×10^{21} n/cm²) in a shorter irradiation time than AGR-1 or AGR-2. Time-average peak fuel temperatures in the different capsules ranged between 888 and 1418°C.

A key objective of this irradiation was to measure the release of fission gases from failed UCO particles in terms of the release-to-birth ratio per failed particle as a function of temperature, burnup, and half-life to establish a correlation that can be used by HTGR designers.^d Because AGR-2 also had one exposed particle in each capsule, those release data can be compared to the measurements from AGR-3/4. In addition, a handful of historic irradiations had very limited but useful data for this comparison. This large amount of release to birth (R/B) data combined from AGR-2 and AGR-3/4 irradiations allows assessment of the effect of isotopic decay constants and fuel temperatures on fission product releases. Details of the analytic approach are found in Reference [14].

Figure 13 plots the R/B per failed particle data from the AGR-3/4 and AGR-2 capsules and a best fit. The R/B values per failed particle for both krypton and xenon isotopes are less than 1% and not sensitive to fuel temperature when fuel temperatures are below 1,050°C. However, when fuel temperature is greater than 1,050°C, the R/B per failed particle values increase exponentially with increasing fuel temperature. The clear downward trend of the fitted lines for AGR-2 and AGR-3/4 R/B data confirms this exponential functional relationship between R/B per failed particle and reciprocal fuel temperature for all isotopes. The 95% confidence bands on the distribution are within a factor of 2.5 of the fitted value, indicating the respectable consistency of R/B per failed particle data given high uncertainties in both fission product release measurement and particle failure estimation.

d. There are other fission product transport objectives in AGR-3/4, including effective diffusion coefficients for metallic fission products in UCO kernels and transport coefficients in compact fuel-matrix and fuel-element graphite. However, these data are not yet available from PIE, which has been underway for about 2 years as of this writing.

The correlation of R/B with isotopic decay constant is a power law with an exponent of n , which represents a slope between $\ln(R_p)$ and $\ln(1/\lambda)$ for isotopes of each gas element (e.g., krypton or xenon) and for any constant fuel temperature. There is no effect of temperature on n values, because n values are similar across AGR-3/4 capsules, which have a wide range of fuel temperatures. The daily n values for AGR-2 and AGR-3/4 irradiations are about 0.3 and stable as a function of irradiation time, indicating no apparent effect of fuel burnup on fission product releases.

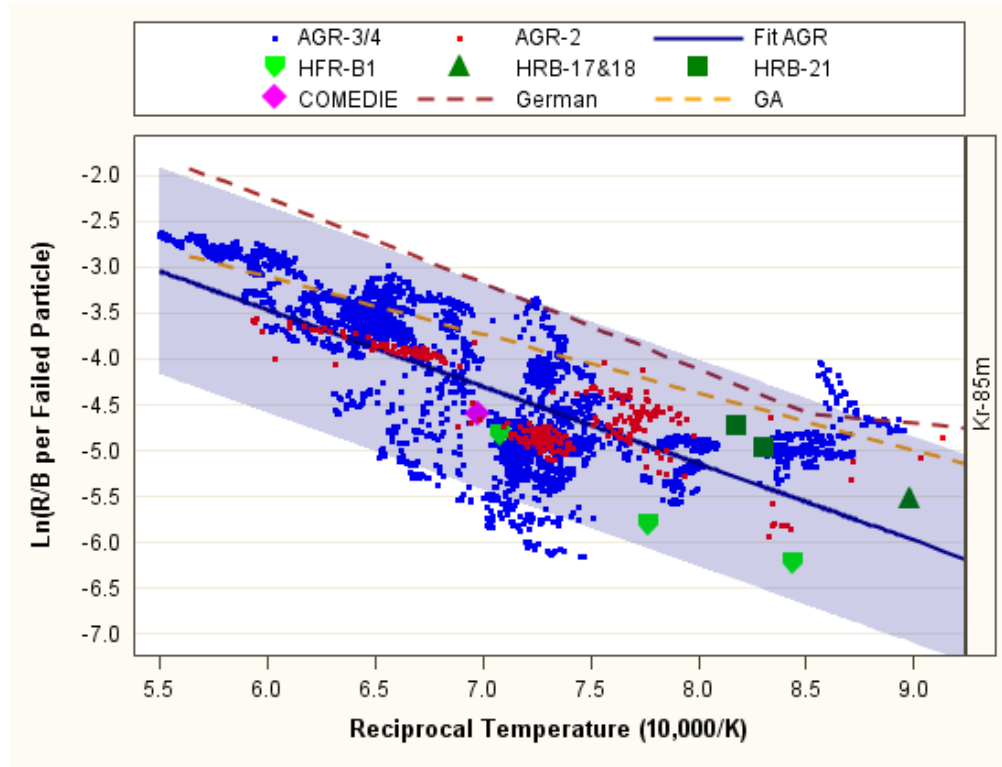


Figure 13. Combined AGR fitted line and R/B per failed particle data for AGR irradiations, historical irradiations, and models (the blue shaded area is 95% bounds of the fitted line).

This analysis, as shown in Figure 13, found that R/B data for AGR-2 and AGR-3/4 test fuel are consistent with each other and complementary. They are also comparable to R/B obtained in historic tests (HFR-B1, HRB-17/18, HRB-21, and COMEDIE). Also represented in the figure are the German and GA models that predict R/B per failed particle somewhat higher than the correlation based on AGR-2 and AGR-3/4 data (i.e., the German model for the entire temperature range and the GA model for lower temperatures). The R/B correlation, as measured during AGR-3/4, can be used by reactor designers to estimate fission gas release from postulated failed fuel in HTGR cores, which is the need for source term calculations for HTGR.

4.3 AGR-5/6/7

AGR-5/6/7 is an instrumented lead-type experiment with online active temperature control and fission product monitoring of the effluent gas. AGR-5/6/7 functions as both the fuel qualification irradiation (AGR-5/6) and a margin irradiation (AGR-7) for the industrially produced UCO TRISO-coated particle fuel developed by the AGR program. Like AGR-3/4, AGR-5/6/7 will be irradiated in the northeast flux trap (NEFT) position in ATR, which is in contrast to the large B positions used to irradiate AGR-1 (B-10) and AGR-2 (B-12). The key irradiation and test configuration parameter specifications are shown in Table 9.

Table 9. AGR-5/6/7 irradiation test specifications.

Parameter	AGR-5/6 Specification	AGR-7 Specification
Instantaneous peak temperature for each capsule (°C)	≤1800	≤1800
Time average temperature distribution goals (°C)	≥600 and <900 for about 30% of fuel ≥900 and <1050 for about 30% of fuel ≥1050 and <1250 for about 30% of fuel ≥1250 and <1350 for about 10% of fuel	Not specified
Time average, peak temperature goal (°C) (for one element)	1350 ± 50	1500 ± 50
Time average, minimum temperature goal (°C)	≤700	Not specified
Minimum compact average burnup (% FIMA)	>6 for all compacts	>6 for all compacts
Maximum fuel compact average burnup (% FIMA)	>18 for at least one compact	>18 for at least one compact
Maximum fuel compact fast neutron fluence (n/m ² , E > 0.18 MeV)	≥ 5.0 × 10 ²⁵ for at least one compact and ≤ 7.5 × 10 ²⁵ for all compacts	≥ 5.0 × 10 ²⁵ for at least one compact and ≤ 7.5 × 10 ²⁵ for all compacts
Minimum fuel compact fast neutron fluence (n/m ² , E > 0.18 MeV)	> 1.5 × 10 ²⁵	> 1.5 × 10 ²⁵
Instantaneous peak power per particle (mW/particle)	≤400	≤400

The overall concept for the AGR-5/6/7 is similar to previous AGR experiment capsules. AGR-5/6/7 will reuse AGR-3/4 design concepts as much as practicable. Cross sections of the AGR-5/6/7 experiment capsules are shown in Figure 14. A horizontal view of the test train is shown in Figure 15. Unlike the previous AGR irradiations, the test train for the AGR-5/6/7 experiment will contain five capsules in different combinations of irradiation temperature and fuel burnup that more broadly span the temperature and burnup range expected in a modular HTGR to provide more representative data on TRISO fuel performance. For AGR-5/6, 30% of the particles will operate at <900°C, 30% will operate at 900°C-1050°C, 30% will operate at 1050 to 1,250°C, and the remaining 10% will operate at 1,250 to 1,350°C. For the margin test, AGR-7, the particles will operate at 1,350 to 1,500°C. AGR-5/6/7 will utilize the full 1.2-m active core height in ATR to provide the desired broad range of fuel burnup and temperature combinations. As shown in Table 9, the fuel compact burnup goals are a minimum of 6% FIMA and a maximum of 18% FIMA. To attain these goals and still be able to control the temperature in the capsules, two packing fractions of compacts will be used in the test train. Compacts with a 40% packing fraction will be used in Capsules 1 and 5 of the test train, and compacts with 25% packing fraction will be used in Capsules 2, 3, and 4.

To achieve the desired statistical relevance, AGR-5/6 will contain approximately 500,000 fuel particles and AGR-7 (margin test) will contain approximately 50,000 fuel particles. Capsule 1 (bottom capsule in test train), contains 10 fuel stacks (90 compacts), has a hollow center to reduce total energy deposition, is 9 in. long, and has no through tubes. With no through tubes, there is more room for fuel stacks; therefore, Capsule 1 contains the most fuel (60%) of the AGR-5/6 capsules and is also the hottest. The purpose of the through tubes is to allow gas lines and instrumentation from lower capsules to be passed up and out of the test train. This means that the capsules are not completely sealed off from one another, but because there is no need for through tubes in Capsule 1, it is completely sealed (no cross-talk between capsules). Because high temperatures degrade instrumentation lines, it makes sense to make Capsule 1 the hottest of the AGR-5/6 capsules. Capsules 2, 4, and 5 have four fuel stacks each and, like Capsule 1, have hollow centers. Capsule 2 and 8 in. long and contains 32 compacts. Capsules 4 and 5 are

6 in. long, and each contains 24 compacts. Capsule 3 (AGR-7 margin test) contains three fuel stacks consisting of 24 compacts and is 8 in. long. It also contains a unique design feature in that the graphite holder has been separated into two pieces, depicted by the two shades of gray in Figure 14, allowing the center mass to run hot while keeping the through tubes relatively cool, thereby extending the life of the instrumentation lines contained within the through tubes.

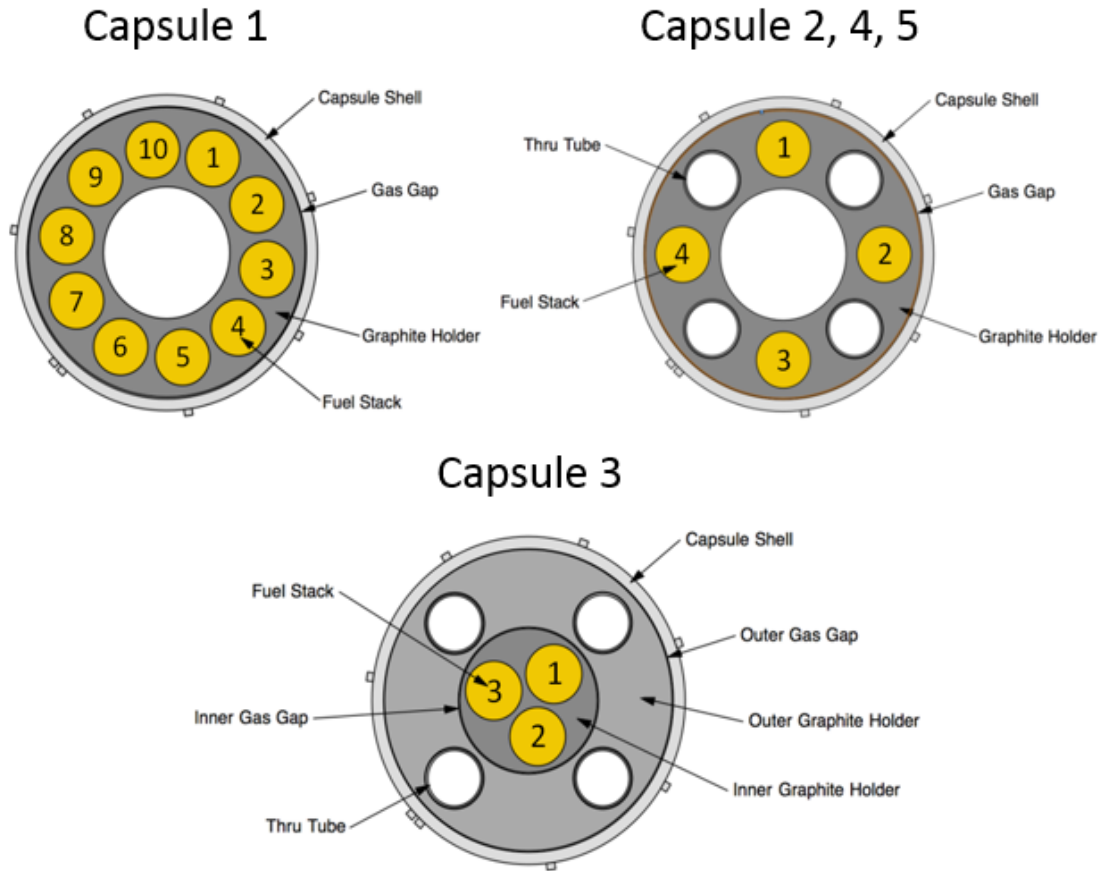


Figure 14. AGR-5/6/7 capsules cross section.

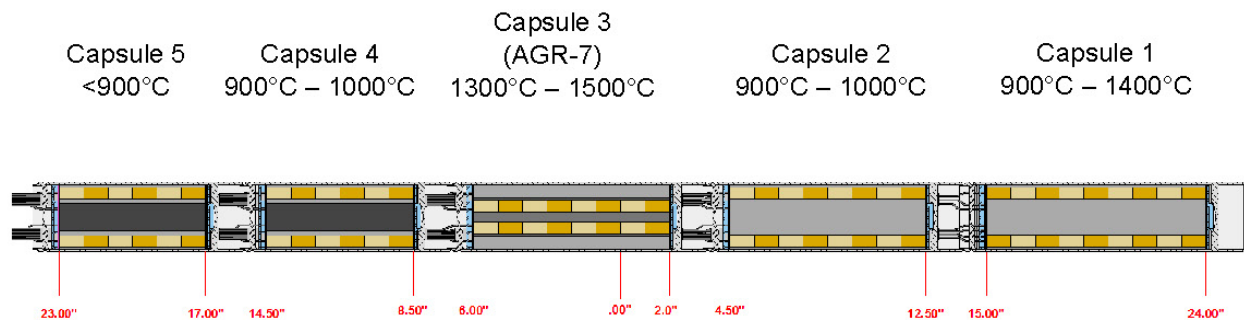


Figure 15. AGR-5/6/7 test train in-core section.

The AGR-5/6/7 experiment test train will be very similar to AGR-3/4, with the five separate stacked capsules welded together to form the core section of the test train. The plenum regions between capsules have been extended over previous designs to accommodate the bending of larger and stiffer

thermocouples. The core section is welded to an umbilical tube (i.e., termed a leadout at ATR) that houses and protects the gas lines and thermocouple leads. The leadout is routed from the NEFT position straight up from the ATR core to the experiment penetration in the reactor vessel top head. Above the vessel top head, the gas lines and thermocouple leads are connected to their facility counterparts in the temperature monitoring, control, and data-collection systems similar to the other AGR experiments.

To maximize the available irradiation space and meet the fluence and burnup requirements, a new flux trap irradiation housing has been designed. The irradiation housing interfaces with the ATR core structure that supports the ATR fuel elements surrounding NEFT; the housing also locates the test train in the center of NEFT. The neutron flux is moderated to reduce the fast-to-thermal neutron flux ratio to prevent excessive fast neutron damage while achieving the desired fuel burnup. The housing also helped lower the overall thermal neutron flux rate to keep the irradiation acceleration factor to less than 3 and prevent possible premature fuel particle failures. The irradiation housing for AGR-5/6/7 consists of inner and outer stainless-steel shells with a hafnium filter sandwiched between them. Three different filters will be used during the irradiation: a heavy filter, an intermediate filter, and a light filter. The appropriate filter will be used based on the anticipated power in the ATR and the fissile content of the test train. The use of three filters will aid in tailoring the fast/thermal spectrum over a much wider operating band.

As in previous AGR experiments, the radioactive content of the gas lines will be measured using a series of gross and high-resolution gamma spectrometers to provide a near real-time measurement of fuel performance during irradiation.

4.4 Uncertainty Considerations

Performing real-time measurements of service conditions during irradiation testing of TRISO fuel is challenging given the high temperatures and long duration of the experiments in ATR. Experimental sensors have been used with some success. AGR-5/6/7 will incorporate a number of new sensors that may provide additional real-time information on key design service conditions in the irradiation (temperature, fission rate/burnup, and fast fluence). Flux wire measurements from the experiment also provide information on thermal and fast fluences after the experiment. Burnup has been measured by gamma scanning of compacts and dissolution of a few kernels from particles [18,19].

Beyond measurements, the AGR program has devoted significant effort to calculations of heat rates, burnup, fluence, and temperatures in the irradiation capsules. Extremely detailed Monte Carlo calculations incorporating each particle and corresponding finite element thermal analysis are used to provide local estimates of heat rates, burnup, fluence, and temperature. The calculation results have been compared to the experimental data when available. Physics calculations for AGR-1 indicate excellent agreement between calculated and measured burnups and fast fluences within +/- 5%. AGR-2 data also indicate excellent agreement. Detailed axial flux wires from AGR-3/4 compare very well with Monte Carlo estimates of the axial flux profile [20]. Temperature calculations are generally within 50 to 75°C of thermocouple measurements, but drift and changes in gaps due to dimensional change of the graphite make detailed comparisons more problematic toward the end of irradiation. An uncertainty analysis has been performed [21] of the temperature estimates for AGR-1, -2, and -3/4 using a formal uncertainty propagation protocol that considers the traditional uncertainties of each key variable used in the calculation but also includes first-order cross-correlation effects of the key variables in the uncertainty estimates. The uncertainties in predicted temperatures using this approach change over the course of the irradiation, because uncertainties in key inputs (like gap size due to graphite shrinkage) increase with time (fast fluence) and the fuel heat rate changes due to fissile burnup and changes in ATR operation. The uncertainties also vary by capsule and experiment given the different gas gap sizes used in each capsule but generally range from 25 to 100°C at one standard deviation. The results also identify those input parameters that have the greatest impact on the overall uncertainty, which has been helpful in designing the follow-on capsules.

5. POST-IRRADIATION EXAMINATION AND SAFETY TESTING

The objective of the PIE and safety testing is to characterize and measure the performance of TRISO fuel after irradiation and during postulated accident conditions. These activities also support the fuel development effort by providing feedback on the performance of kernels, coatings, and compacts. Data from PIE and accident testing in combination with the in-reactor measurements will provide the data necessary to demonstrate compliance with fuel performance requirements and to support the development and validation of computer codes. PIE of UCO TRISO fuel irradiated in AGR-1 is complete, and similar work for AGR-2 is underway. The PIE was focused on evaluating fuel performance during irradiation and during post-irradiation high-temperature heating tests in helium. Key aspects of fuel performance that were investigated were fission product release from particles and compacts, and radiation-induced changes in kernel and coating microstructures. Safety tests were performed by heating the fuel compacts in helium at temperatures of 1,600, 1,700, or 1,800°C, with nominal hold times of 300 hours. The results are discussed here.

5.1 Fission Product Distributions

A mass balance of fission products was performed by quantifying the fission product content in the various components of all six irradiation capsules (representing the inventory released from the fuel compacts during irradiation) and within the matrix of eight compacts (representing the inventory released from particles but retained in the compact outside of the SiC layer during irradiation). The results are presented graphically in Figure 16, showing the range of inventory fractions (based on either single compacts or all 12 compacts in a single capsule, as appropriate) found in the compacts and the irradiation capsules. Very low release of key metallic fission products (except silver) confirms the excellent performance measured under irradiation and demonstrates the robustness of the SiC layer as a barrier to fission product release [22,23].

As indicated in Figure 16, the cesium release from the fuel was very low. In compacts with no particles exhibiting a failed SiC layer, the Cs-134 fractional inventory in the matrix was $<2\text{E}-05$, and in capsules containing zero particles with failed SiC, the Cs-134 fractional release from the compacts was $<3\text{E}-06$. Releases of Sr and Eu into the compact matrix were generally small ($\sim 1\text{E}-06$ to $1\text{E}-02$), indicating some diffusion through the coatings. Ce-144 releases to the compact matrix were a factor of 10 smaller ($\sim 1\text{E}-06$ to $1\text{E}-03$). However, the amount of these materials in the capsule components (graphite holder, end caps, and steel shell) tends to be much less compared to what is present in the compact matrix (compare the “compacts” and “capsule” data in Figure 16), demonstrating good retention in the matrix.

The level of Pd found outside the SiC was approximately 1% in the five compacts analyzed. Despite this large amount of Pd in the fuel matrix, no widespread Pd corrosion or attack of SiC has been observed during metallographic examination of a number of as-irradiated TRISO particles. This was unexpected, because Pd attack of SiC at high burnup in TRISO fuel has been postulated as a potential failure mode [24].

Silver release was high and varied significantly from compact to compact as a result of the differences in the temperatures experienced by each compact under irradiation.

Particles that experienced SiC failure during the AGR-1 irradiation were identified, as detailed later in this report. It is estimated that a total of four particles in the entire AGR-1 test train experienced a SiC failure under irradiation. This corresponds to an in-service SiC failure fraction of $3.1\text{E}-05$ at 95% confidence. There is no specification for in-service SiC failures. However, this value is a factor of 7 below the incremental in-service full TRISO failure fraction of $2\text{E}-04$. Furthermore, gamma counting of two of the particles with failed SiC using the Advanced Irradiated Microsphere Gamma Analyzer indicated significant cesium retention after irradiation (~ 30 to 60%), which is much higher than predicted using German cesium diffusivities in kernel and PyC layers.

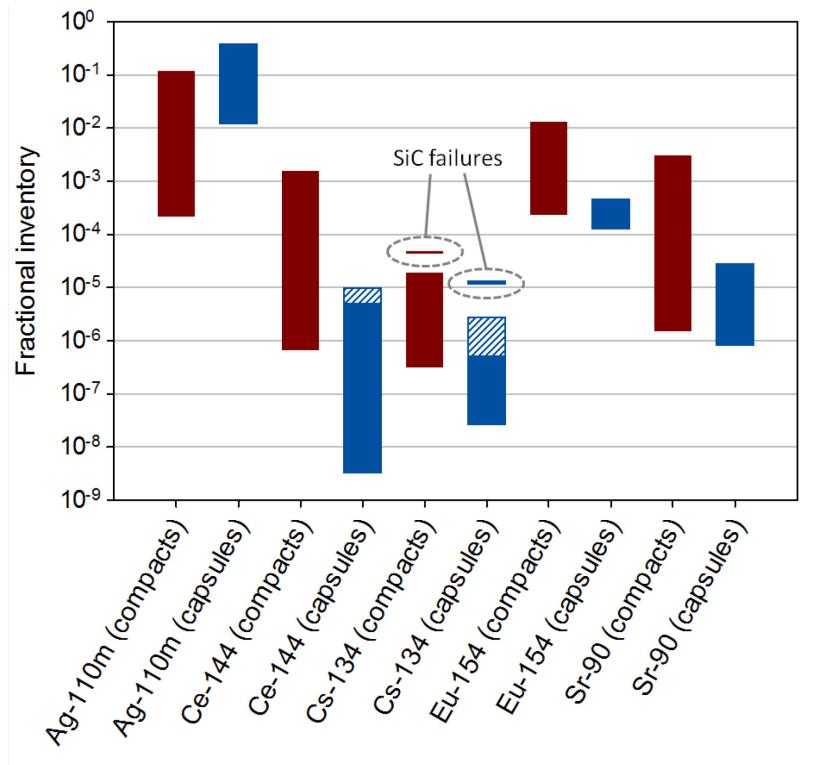


Figure 16. Range of fractional fission product inventories found in the matrix of examined compacts (red columns) and on the irradiation capsule components (blue columns). Instances where compacts and capsules contained SiC failures are indicated separately on the plot. Hashed areas indicate that the measured values on some capsule components were above the detection limit of the techniques; therefore, the sum of contributions from all components represents a conservative upper bound for the total inventory in several of the capsules.

5.2 Irradiated Fuel Particle Microstructural Evolution

Extensive microscopic examination of particle cross sections was performed. This included numerous cross sections of select intact as-irradiated compacts [25] as well as loose particles deconsolidated from numerous as-irradiated or safety-tested compacts [26]. In addition, a select number of particles were analyzed with nondestructive x-radiography with 3D tomographic reconstruction. Common features in the irradiated particles included densification of the buffer layer and swelling of the kernel with related formation of gas-filled bubbles (Figure 17). There was no detectable high-burnup kernel migration (the so-called “amoeba effect”), indicating the efficacy of the UCO fuel in limiting the oxygen partial pressure in the fuel and the formation of carbon monoxide.

In the majority of particles, the buffer layer debonded from the IPyC layer. This was observed as either complete (Figure 17a) or partial (Figure 17b) debonding in the polished plane analyzed. Much less common were particles in which the buffer and IPyC layers remained completely bonded in the plane observed (Figure 17c), where the buffer densification resulted in the inner diameter increasing while the kernel swelled to filled the increasing volume. Such particles constituted 4% of approximately 1,000 particles observed in a study of compact cross sections.

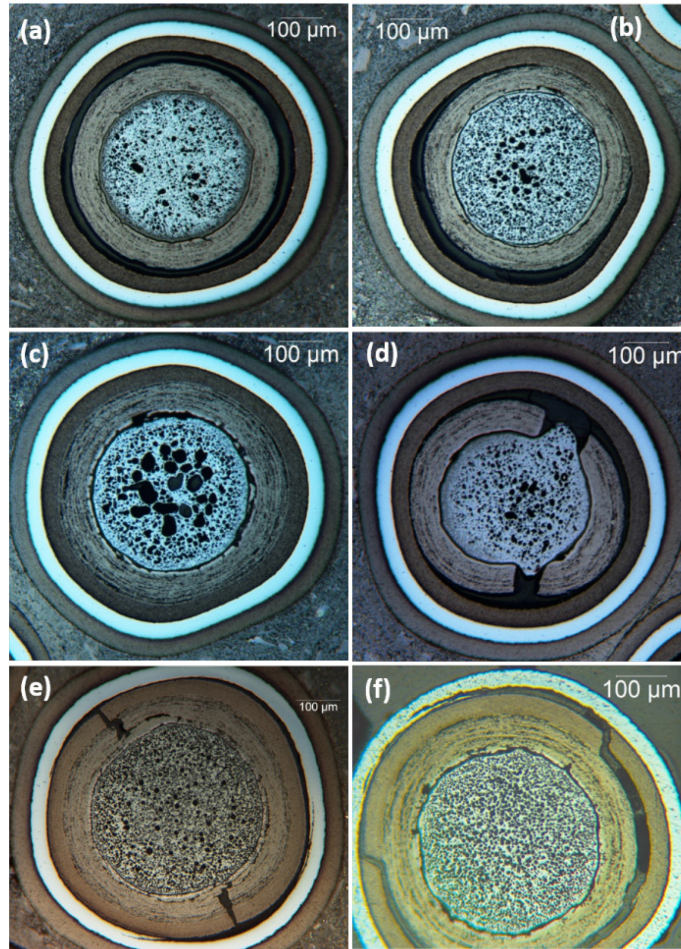


Figure 17. Examples of various AGR-1 irradiated particle microstructures (from Reference [27]).

Fracture of the buffer layer was common (observed in 23% of particles studied in the compact cross sections), and these were often accompanied by expansion of the kernel into the gap formed at the point of fracture (Figure 17d). While particles with the representative microstructure shown in Figure 17d were fairly common, there appeared to be no obvious detrimental effects on the outer, dense coating layers, even in cases where the kernel was in direct contact with the IPyC layer. On the other hand, if the buffer-IPyC interface remained intact, as shown in Figure 17c, fracture of the buffer layer was always accompanied by fracture of the IPyC layer and often also included debonding of the IPyC from the SiC layer (Figure 17e).

Fracture of the buffer layer was not always necessary for IPyC fracture to occur. In some particles, partial debonding of the buffer-IPyC layer apparently led to development of sufficient stress in the IPyC layer to cause fracture (Figure 17f), often with resultant debonding between the IPyC and SiC layers and, in rare cases, partial fracture of the SiC at the IPyC-SiC interface (as shown in Figure 17f) that did not lead directly to SiC failure. Because partial buffer-IPyC debonding (Figure 17b) was much more common than no debonding (Figure 17c), this type of IPyC fracture was more common than the type shown in Figure 17e. Subsequent detailed analysis of particles with failed SiC layers [25] revealed that most exhibited buffer-induced IPyC fracture like that shown in Figure 17e or Figure 17f. This fracture then allowed concentration of fission products at the inner SiC surface in the vicinity of the IPyC-SiC debond, which subsequently attacked the SiC layer, eventually penetrating the layer and causing a loss in retention of fission products such as cesium. An important conclusion from this analysis is that low-stress buffer-IPyC debonding appears to be a desirable condition.

No significant dependence of particle morphology on burnup, fast fluence, or temperature was apparent over the range of irradiation conditions represented by the compacts examined in the AGR-1 PIE. After safety testing, similar particle morphologies were generally observed, although instances of SiC failure increased.

5.3 Safety Testing

Post-irradiation accident simulation heatup testing (“safety testing”) of UCO TRISO-coated particle fuel from AGR-1 is demonstrating excellent robustness of the UCO TRISO fuel. An example of fission product release from 1,600°C safety testing is shown in Figure 18 [28]. Very low releases have been measured in safety testing after hundreds of hours at 1,600 and 1,700°C [29]. Summary results for Cs-134 for 15 AGR-1 compacts are shown in Figure 19, which includes results from tests conducted at 1,600, 1,700, and 1,800°C. During safety testing, compact Cs-134 release fractions were $<5 \times 10^{-6}$ if all SiC layers remained intact [29]. This was true in one case even at 1,800°C for ~100 hours, after which a SiC layer failure occurred with corresponding cesium release. On the other hand, compacts in which one or more particles experienced SiC layer failure exhibited Cs-134 releases that rapidly reached a level of 10^{-4} or greater. This Cs-134 release behavior during safety tests is summarized in Figure 19. Note the two distinct populations: compacts with final test release $<5 \times 10^{-6}$ and those $>10^{-4}$ (the fraction equivalent to a single particle inventory in these compacts is 2.4×10^{-4}). The presence of SiC failures in the latter population was confirmed by extensive destructive examination of most of the compacts after the tests, including gamma counting of each individual particle to locate those with low cesium inventory and x-ray tomography to identify SiC degradation in these particles [25]. Overall, Cs-134 release from the compacts was $\leq 2 \times 10^{-4}$ after 300 hours at 1,600°C and about 1 order of magnitude higher after 300 hours at 1,800°C.

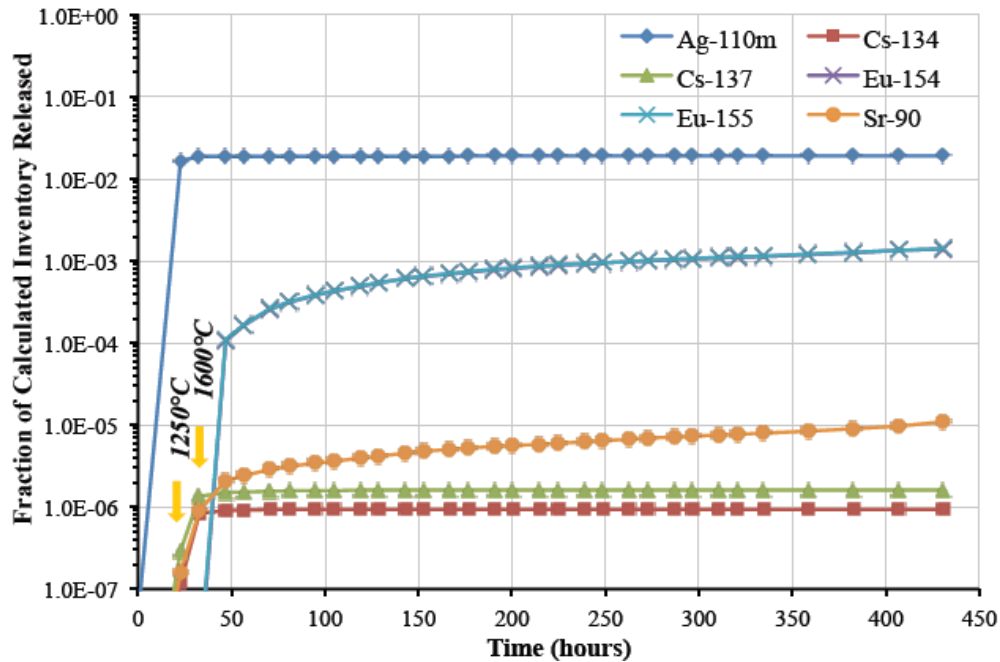


Figure 18. Fission product release from heating of AGR-1 Compact 6-4-3 at 1,600°C.

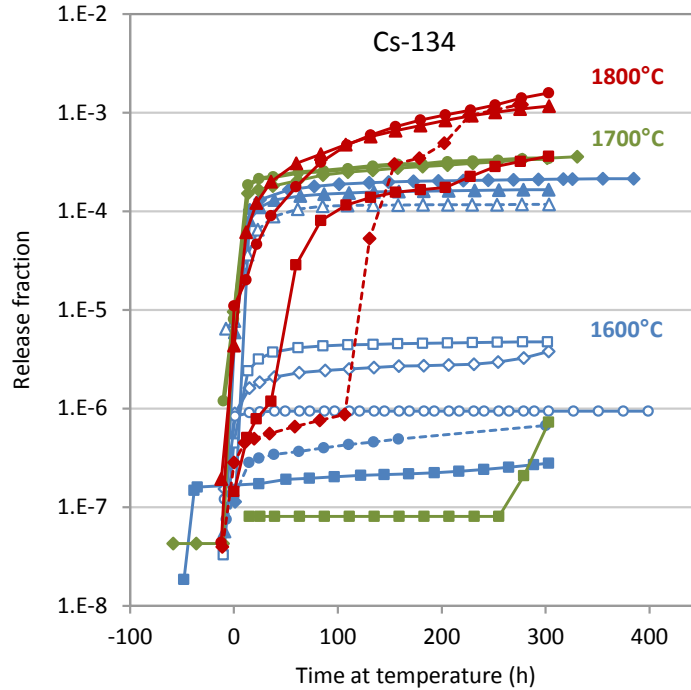


Figure 19. Cs-134 release from AGR-1 compacts heated at 1,600, 1,700, and 1,800°C.

Ag, Sr and Eu were also measured during the accident heating tests [29]. As shown in Figure 20, silver releases vary between ~ 0.4 and 34% of the total inventory in the fuel compact, and the results indicate that this is predominantly due to fission products that resided in the matrix at the end of irradiation.

Strontium and europium releases are in the range of $8E-6$ to $1E-3$ and $3E-4$ to $3E-3$, respectively, after 300 hours at either 1,600 or 1,700°C and 1% after 300 hours at 1,800°C. At these temperatures, it is difficult to discern if there are any releases from the particles during high-temperature heating, because it appears that there is a significant contribution from fission products that diffused into the matrix during the irradiation. It is important to note that the 300 hours of high-temperature testing is well in excess of that expected in a modular HTGR where temperatures of 1,600°C are experienced for only about 25 to 40 hours. Furthermore, only about 2 to 3% of the compacts in the modular HTGR core experience these high temperatures during the postulated depressurized loss-of-forced-circulation heatup event. Thus, because the expected number of compacts that will experience relatively short times at high temperatures is small, core-wide releases of these fission products during a modular HTGR core heatup event will be very low.

The behavior at 1,800°C for the UCO TRISO is worthy of mention. While SiC failures are evident in Figure 19, they represent only a small fraction of the inventory in the fuel compact. By comparison, an 1,800°C heating test of German UO₂ TRISO fuel produced tens of percent release of cesium by 300 hours [30]. The reason for this outstanding behavior of UCO at 1,800°C is under active study but may be due to the lack of CO produced in the fuel kernel as compared to UO₂, which can attack SiC at high temperature [31].

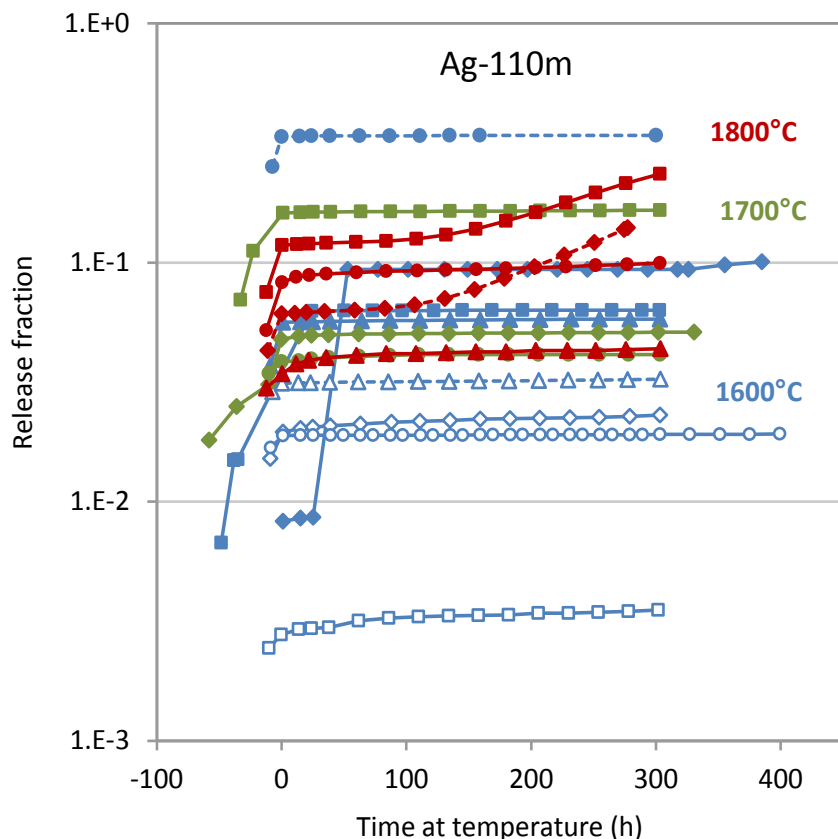


Figure 20. Ag-110m fractional release from AGR-1 compacts during safety tests. Test temperature is indicated by the color coding shown in the figure. Note the increase in release fraction for two of the 1,800°C tests (in red) after ~100 hours at 1,800°C.

In summary, no full TRISO particle failures (no measured noble gas release) were observed in accident heating tests of AGR-1 compacts at 1,600 or 1,700°C. This corresponds to a 95% failure fraction of $\sim 6.6\text{E}-05$, a factor of 8 below the HTGR prismatic reactor specification. Fission product release from UCO TRISO fuel is very low at 1,600, 1,700, and 1,800°C unless a SiC layer fails due to either a manufacturing defect or a radiation-induced failure mechanism. Cs releases after 300 hours at 1,600°C tend to be $< 1\text{E}-05$ from compacts containing only intact particles. For cases where a SiC failure occurs, releases tend to be around 1 to $2\text{E}-04$ (100% release from one particle corresponds to a release fraction of $2.4\text{E}-04$) and are dependent on the total number of SiC failures that occurred. The best estimate of SiC failures observed during heating at 1,600°C is three out of about 33,000 particles, which corresponds to $\leq 2.4\text{E}-04$ at 95% confidence. Although there is no specification for in-service SiC failures under accident conditions, this value (somewhat limited by the testing statistics—only eight compacts) is still a factor of 2 below the incremental in-service full-TRISO failure fraction of $6\text{E}-04$. Post-test analysis using the Advanced Irradiated Microsphere Gamma Analyzer on one particle that exhibited SiC failure during safety testing has indicated cesium retention of 30 to 60% [29]. Thus, even if the SiC fails under high-temperature heating, not all of the cesium is released.

Similar heatup testing has begun on AGR-2 compacts [32]. Figure 21 plots the fission product release measured from Compacts 5-2-2 and 2-2-2. The Cs release from both compacts was very low, less than $6\text{E}-06$ after 300 hours at 1,600°C. Post-test destructive leaching confirmed no TRISO failures. The Ag, Eu and Sr releases were similar to those seen in AGR-1 and are attributed to release of those isotopes that had diffused through intact TRISO particle into the matrix under irradiation. The higher Eu and Sr

releases from Compact 2-2-2 are due to the greater matrix inventory, since the compacts in Capsule 2 in AGR-2 were irradiated near 1,400°C, which is 150°C greater than the irradiation temperature for Capsule 5. Thus, the safety behavior for AGR-2 produced fuel from a large coater is similar to the laboratory-scale fuel produced for AGR-1. More recent, but as yet unpublished, preliminary results from other AGR-2 compacts show similar behavior.

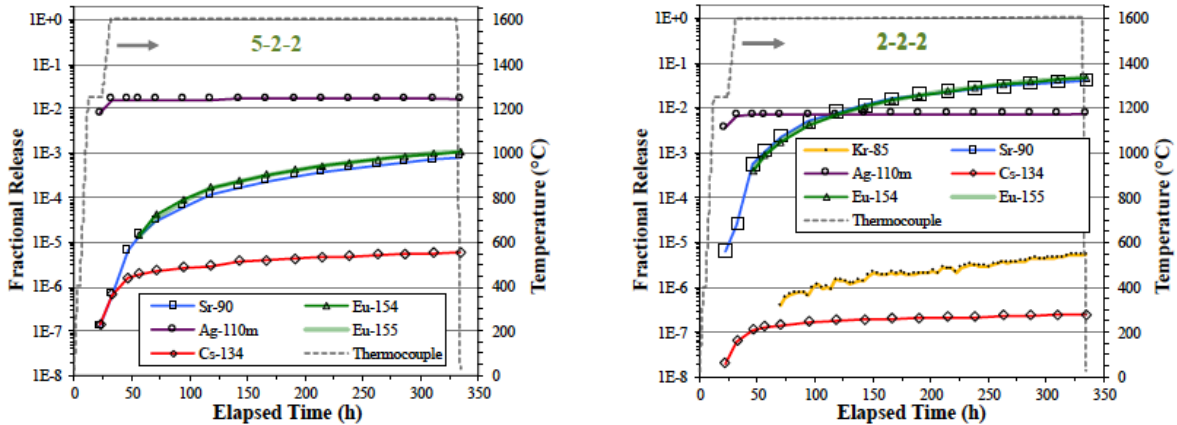


Figure 21. Fission product release results from AGR-2 Compacts 5-2-2 and 2-2-2 under high-temperature accident heating.

5.4 SiC Failure Mechanisms

Particles that experienced SiC layer failure during irradiation or during safety tests were identified based on elevated cesium release, and many of these were analyzed in detail—both nondestructively—using x-ray imaging with tomographic reconstruction and by cross sectioning and microanalysis using a number of analytical characterization methods [25]. For SiC failures during irradiation, the examination process started with gamma-scanning the empty graphite fuel holders to locate regions with elevated cesium activity [27]. The compacts that were adjacent to these regions during irradiation were identified as likely to contain one or more particles that experienced SiC failure in-pile. These as-irradiated compacts, as well as compacts that exhibited Cs release during safety testing indicative of SiC failure, were then deconsolidated to liberate the particles, which were all gamma counted to quantify the inventory of Cs-137, Cs-134, and Ce-144. Particles that exhibited abnormally low cesium inventory were then collected, and x-ray imaging was used to nondestructively observe the interior particle morphology.

In total, three particles with high cesium release during irradiation were found and examined (a fourth particle was detected during deconsolidation-leach-burn-leach analysis of another compact but was destroyed in the process and therefore not subjected to detailed microstructure analysis). In all of these particles, a similar failure mechanism was implicated. Buffer shrinkage resulted in IPyC fracture due to incomplete debonding at the buffer-IPyC interface. In one case, an arrowhead-like fracture occurred (similar to that shown in Figure 17e), while in the other two particles, IPyC fracture was related to stress from the buffer pulling away from the IPyC (similar to Figure 17f). The IPyC fracture then exposed the SiC layer to concentrated chemical attack of fission products (notably palladium), which caused degradation through the entire layer (Figure 22). It is noteworthy that significant attack of the SiC layer was never observed in particles without this sort of IPyC fracture or in these three particles in areas away from the IPyC fracture. So while these failures were ultimately caused by Pd attack on SiC, prior fracture of the IPyC layer appears to be a prerequisite for the attack to occur.

Safety testing produced SiC failures in fractions higher than during irradiation, with the failure fractions increasing with test temperature. At 1,600°C, two of the three particles with SiC failures that were identified were examined in detail, and the cause of the SiC failure was determined to be an

as-fabricated defect in the SiC layer (the third particle was not recovered for analysis). At 1,700 and 1,800°C, nearly all of the particles recovered exhibited a similar SiC failure mechanism to the one identified for the as-irradiated particles. The major differences were that the elevated temperature increased the severity of the SiC degradation due to enhanced reaction with fission products.

The dominant SiC failure mechanism described here is significantly different from that currently embedded in fuel performance models, including the code PARFUME (PARTicle FUel ModEl). Incorporation of this failure mode into the models is likely to be challenging due to its complex nature (essentially a two-part mechanism involving thermomechanical behavior of the buffer and IPyC under irradiation, followed by focused chemical attack of the SiC layer) and a lack of some key data (including buffer strength, buffer-IPyC bond strength, fission product partitioning coefficients at the site of the IPyC fracture, and reaction kinetics for the chemical degradation).

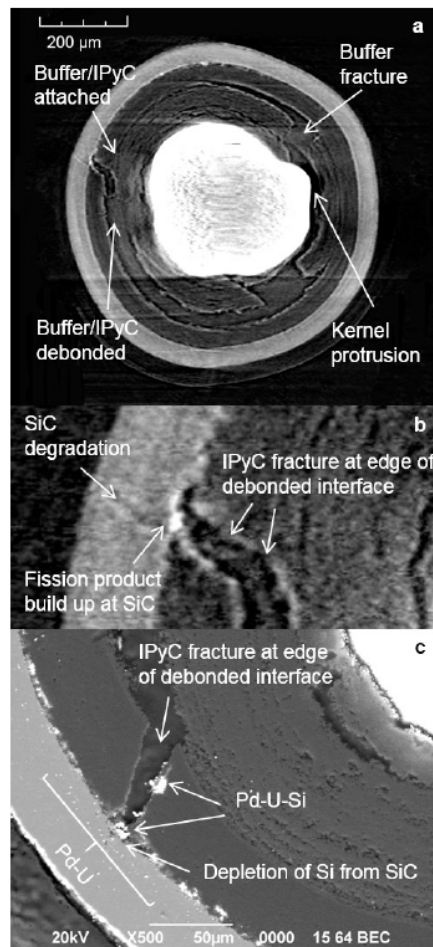


Figure 22. (a) X-ray tomogram showing microstructure in as-irradiated Compact 5-2-3 particle that led to SiC failure and cesium release; (b) x-ray close-up of degraded pathway through SiC; and (c) scanning electron microscope micrograph of degraded region with energy dispersive x-ray spectroscopy identification of Pd and U in the SiC and Si outside the SiC.

6. FUEL PERFORMANCE MODELING

The AGR program has developed a fuel performance model called PARFUME. The code calculates the thermo-mechanical response of the TRISO coatings and the physio-chemical behavior of the kernel, including fission gas release, CO production in the case of a UO₂ kernel, kernel migration, and Pd attack

of the SiC layer, under normal and accident conditions. The code also calculates the release of fission products from TRISO-coated particle fuel. Because the timeframe for development of the code was before UCO TRISO particles had been irradiated and safety tested, the phenomena modeled in the code are based entirely on past UO₂ TRISO fuel in U.S. and Germany. The code has been a part of three major benchmarking activities [33,34]: a thermo-mechanical benchmark performed as part of an International Atomic Energy Agency coordinated research program, a fission product release benchmark under the same program, and a more recent fission product release benchmark including results from the AGR program.

The PARFUME code was used to predict the release of fission products silver, cesium, and strontium from AGR-1 fuel particles and compacts during irradiation [35] using the volume average temperature for each of the 620 days of irradiation. PARFUME-predicted fractional release of silver, cesium, and strontium was determined and compared to PIE measurements on release of these fission products from fuel compacts and fuel particles, and retention of silver in the compacts outside of the silicon carbide (SiC) layer. For silver, comparisons show a trend of under-prediction at low burnup and over-prediction at high burnup. PARFUME has limitations in the modeling of the temporal and spatial distributions of the temperature and burnup across the compacts, which affects the accuracy of its predictions. Nevertheless, the comparisons on silver release lie in the same order of magnitude. Results show an overall over-prediction of the fractional release of cesium by PARFUME. For particles with failed SiC layers, the over-prediction is by a factor of up to 3, corresponding to a potential over-estimation of the diffusivity in UCO by a factor of up to 250. For intact particles, whose measured release is much lower, the over-prediction is by a factor of up to 100, which could be attributed to an over-estimated diffusivity in SiC by about 40% on average. The release of strontium from intact particles is also over-predicted by PARFUME, which also points toward an over-estimated diffusivity of strontium in either SiC or UCO, or possibly both. The measured strontium fractional release from intact particles varied considerably from compact to compact, making it difficult to assess the effective over-estimation of the diffusivities. Furthermore, the release of strontium from particles with failed SiC is difficult to observe experimentally due to the release from intact particles, preventing any conclusions to be made on the accuracy or validity of the PARFUME predictions and the modeled diffusivity of strontium in UCO.

The PARFUME code was also used to predict the release of fission products silver, cesium, strontium, and krypton during 15 AGR-1 safety tests at temperatures ranging from 1,600 to 1,800°C [36]. Comparisons between PARFUME predictions and PIE results of the safety tests were conducted on two types of AGR-1 compacts: compacts containing only intact particles and compacts containing one or more particles whose SiC layers failed during safety testing. In both cases, PARFUME globally over-predicted the experimental release fractions by several orders of magnitude: more than 3 (intact SiC) and 2 (failed SiC) orders of magnitude for silver, more than 3 (intact SiC) and up to 2 (failed SiC) orders of magnitude for strontium, and up to 2 (intact SiC) and more than 1 (failed SiC) orders of magnitude for krypton. The release of cesium from intact particles was also largely over-predicted (by up to 5 orders of magnitude), but its release from particles with failed SiC was only over-predicted by a factor of about 3. These over-predictions can be largely attributed to an over-estimation of the diffusivities used in the modeling of fission product transport in TRISO-coated particles that are based on international consensus estimates, as discussed in Reference [37]. The integral nature of the release data makes it difficult to estimate the individual over-estimations in the kernel or each coating layer. Nevertheless, a tentative assessment of correction factors to these diffusivities was performed to enable a better match between the modeling predictions and the safety testing results. The method could only be successfully applied to silver and cesium. The diffusivity of silver in SiC appears to be over-estimated by factors of about 1,000 at 1,600 and 1,700°C, and 100 at 1,800°C. After accounting for the over-prediction under irradiation, PARFUME calculations were used to estimate the magnitude of the over-estimation of the diffusivity of cesium in UCO. The overestimate of the diffusivity of cesium in UCO ranges from 25 to 250 at 1,600°C, from 1,500 to 10,000 at 1,700°C, and from 300 to 1,000 at 1,800°C. In the case of strontium, correction factors could not be assessed, because potential release during the safety tests could not be distinguished

from strontium in the matrix that was released during irradiation. In the case of krypton, all the coating layers are partly retentive and the available data did not allow the level of retention in individual layers to be determined, hence preventing derivation of any correction factors.

7. LICENSING IMPLICATIONS

The results of the AGR program have been very successful to date, and they support current safety design and analysis assumptions about fuel performance and radionuclide retention required under the U.S. modular HTGR licensing strategy.

Fabrication of high-quality low-defect fuel is achievable at industrial scale. There is an improved understanding of the TRISO fuel fabrication process and improved fabrication and characterization of TRISO fuel produced by the fuel vendor. Defect fractions on the order of 10^{-5} are achievable. The process produces narrow distributions of fuel attributes (e.g., standard deviation of coating thicknesses and densities are small). The process is stable and repeatable at industrial scale (batch-to-batch variation is very small).

The AGR program has demonstrated excellent irradiation performance of a large statistical population of UCO TRISO fuel particles under high-burnup, high-temperature modular HTGR conditions (both AGR-1 and AGR-2). This outstanding performance results in low release of fission products to the helium coolant.

PIE of AGR-1 indicates large Ag releases from the TRISO fuel, low releases of Cs ($<2E-5$), and low releases of Sr and Eu ($\sim 1E-6$ to $1E-2$) from intact particles under irradiation. Significant retention was observed in the fuel matrix and graphite. No widespread Pd attack or corrosion of SiC was observed despite finding large amounts of Pd outside of the SiC layer.

Safety testing at 1,600 and 1,700°C is demonstrating robustness of UCO TRISO under depressurized conduction cooldown conditions. No full TRISO particle failures have been observed at 1,600 or 1,700°C. Release of cesium from intact particles at 1,600°C is $<5E-6$. When a SiC layer in a particle failed, some of the Cs from that particle was released. Releases of Ag, Sr and Eu at 1,600 and 1,700°C are attributed to diffusion of these fission products into the fuel matrix during irradiation and subsequent release from the matrix upon high-temperature heating. Overall, the results indicate low incremental release of safety-relevant fission products under accident conditions. These results obtained to date from AGR-2 UCO fuel produced at engineering scale are similar to that from AGR-1 laboratory-scale fuel.

Models using the historical database significantly over-predict the releases of key fission products during irradiation and high-temperature accident heating.

Collectively, these irradiation and accident safety testing results provide a high level of confidence that the AGR program will successfully demonstrate the superior performance capability of TRISO fuel required by the modular HTGR safety design.

8. REFERENCES

-
- [1] J. Simonds, "Technical Program Plan for INL Advanced Reactor Technologies Technology Development Office/Advanced Gas Reactor Fuel Development and Qualification Program," PLN-3636, Rev. 5, Idaho National Laboratory, May 2016.
 - [2] David A. Petti, John Maki, John Hunn, Pete Pappano, Charles Barnes, John Saurwein, Scott Nagley, James Kendall, and Richard Hobbins, "Overview and Status of the DOE Advanced Gas Reactor (AGR) Fuel Development and Qualification Program," *The Journal of The Minerals, Metals, and Materials Society*, September 2010, pp. 62–66.
 - [3] Idaho National Laboratory, *NGNP Fuel Qualification White Paper*, INL/EXT-10-18610, July 2010.

-
- [4] Idaho National Laboratory, *Mechanistic Source Terms White Paper*, INL/EXT-10-17997, July 2010.
- [5] David A. Petti, Richard R. Hobbins, Peter Lowry, and Hans Gougar, “Representative Source Terms and The Influence of Reactor Attributes on Functional Containment in Modular High Temperature Gas-cooled Reactors,” *Nuclear Technology*, Vol. 184, pp. 181–197, November 2013.
- [6] J. Einerson, “Statistical Sampling Plan for AGR Fuel Materials,” EDF-4542, Rev. 4, April 2005.
- [7] W. F. Skerjanc, J. T. Maki, B. P. Collin, and D. A. Petti, “Evaluation of Design Parameters for TRISO-coated Fuel Particles to Establish Manufacturing Critical Limits Using PARFUME,” *Journal of Nuclear Materials*, Vol. 469, 2016, pp. 99–104.
- [8] Scott G. Nagley, Charles M. Barnes, DeWayne L. Husser, Melvin L. Nowlin, and W. Clay Richardson, “Fabrication of Uranium Oxycarbide Kernels for HTR Fuel,” *5th International Topical Meeting on High Temperature Reactor Technology (HTR 2010)*, Prague, Czech Republic, October 18–20, 2010.
- [9] Charles M. Barnes, Douglas W. Marshall, Joe T. Keeley, and John D. Hunn, “Results of Tests to Demonstrate a Six-Inch Diameter Coater for Production of TRISO-Coated Particles for Advanced Gas Reactor Experiments,” *4th International Topical Meeting on High Temperature Reactor Technology (HTR 2008)*, Washington, D.C., October 2008.
- [10] Jeffrey A. Phillips, Eric L. Shaber, Jeffrey J. Einerson, David A. Petti, Scott E. Niedzialek, W. Clay Richardson, and Scott G. Nagley, “Compacting Scale Up and Optimization of Cylindrical Fuel Compacts for the Next Generation Nuclear Plant,” *6th International Topical Meeting on High Temperature Reactor Technology (HTR 2012)*, Tokyo, Japan, October 28–November 1, 2012.
- [11] Douglas Marshall, “Comparative Study of Laboratory Scale and Prototypic Production Scale Fuel Fabrication Processes and Product Characteristics,” *7th International Topical Meeting on High Temperature Reactor Technology (HTR-2014)*, Weihai, China, October 2014.
- [12] S. Blaine Grover, David A. Petti, and John T. Maki, “Completion of the First NGNP Advanced Gas Reactor Fuel Irradiation Experiment, AGR-1, in the Advanced Test Reactor,” *5th International Topical Meeting on High Temperature Reactor Technology (HTR 2010)*, Prague, Czech Republic, October 18–20, 2010.
- [13] S. Blaine Grover and David A. Petti, “Status of the NGNP Fuel Experiment AGR-2 Irradiated in the Advanced Test Reactor,” *6th International Topical Meeting on High Temperature Reactor Technology (HTR 2012)*, Tokyo, Japan, October 28–November 1, 2012.[]
- [14] J. J. Einerson, B. T. Pham, D. M. Scates, J. T. Maki, and D. A. Petti, “Analysis of fission gas release-to-birth ratio data from AGR irradiations,” *Nuclear Engineering and Design*, Vol. 306, pp. 14–23, 2016.
- [15] Blaise Collin, “AGR-1 Irradiation Test Final As-Run Report,” INL/EXT-10-18097, Rev. 3, June 2015.
- [16] Blaise Collin, *AGR-2 Irradiation Test Final As-Run Report*, INL/EXT-14-32277, Rev. 2, August 2014.
- [17] Blaise Collin, “AGR-3/4 Irradiation Test Final As-Run Report,” INL/EXT-15-35550, Rev. 1, May 2016.

-
- [18] James Sterbentz, J. M. Harp, P. A. Demkowicz, G. L. Hawkes, and G. S. Chang, "Validation of the Physics Analysis used to characterize the AGR-1 TRISO Fuel Irradiation Test," Paper 15497, *Proceedings of ICAPP 2015, Nice, France, May 3–6, 2015*.
- [19] Jason M. Harp, P. A. Demkowicz, P. L. Winston, and J. W. Sterbentz, "An Analysis of Nuclear Fuel Burnup in the AGR 1 TRISO Fuel Experiment Using Gamma Spectrometry, Mass Spectrometry, and Computational Simulation Techniques," *Nuclear Engineering and Design*, Vol. 278, 2014, pp. 395-405.
- [20] James Sterbentz, "JMOCUP As-Run Daily Physics Depletion Calculation for the AGR-3/4 TRISO Particle Experiment in ATR Northeast Flux Trap," ECAR-2753, June 5, 2015.
- [21] Binh T. Pham, Jeffrey J. Einerson, Grant L. Hawkes, Nancy J. Lybeck, and David A. Petti, "Impact of Gap Size Uncertainty on Calculated Temperature Uncertainty for the Advanced Gas Reactor Experiments," *8th International Topical Meeting on High Temperature Reactor Technology (HTR-2016), November 2016, Las Vegas, Nevada*.
- [22] Jason M. Harp, Paul A. Demkowicz, and Scott A. Ploger, "Post-irradiation Examination and Fission Product Inventory Analysis of AGR-1 Irradiation Capsules," *6th International Topical Meeting on High Temperature Reactor Technology (HTR 2012), Tokyo, Japan, October 28–November 1, 2012*.
- [23] Paul A. Demkowicz, John D. Hunn, Robert N. Morris, Blaise P. Collin, Jason M. Harp, Philip L. Winston, Charles A. Baldwin, and Fred C. Montgomery, "Preliminary Results of Post-Irradiation Examination of the AGR-1 TRISO Fuel Compacts," *6th International Topical Meeting on High Temperature Reactor Technology (HTR 2012), Tokyo, Japan, October 28–November 1, 2012*.
- [24] J. T. Maki, D. A. Petti, D. L. Knudson, and G. K. Miller, "The challenges associated high burnup, high temperature, and accelerated irradiation for TRISO-coated particle fuel," *Journal of Nuclear Materials*, Vol. 371, 2007, pp. 270–280.
- [25] Scott Ploger, Paul Demkowicz, John Hunn, and J. S. Kehn, "Microscopic Analysis of Irradiated AGR-1 Coated Particle Fuel Compacts," *Nuclear Engineering and Design*, Vol. 271, 2014, pp. 221–230.
- [26] Paul A. Demkowicz, John D. Hunn, Robert N. Morris, Isabella van Rooyen, Tyler Gerczak, Jason M. Harp, and Scott A. Ploger, *AGR 1 Post Irradiation Examination Final Report*, INL/EXT-15-36407, August 2015.
- [27] Paul A. Demkowicz, John D. Hunn, David A. Petti, and Robert N. Morris, "Key results from irradiation and post-irradiation examination of AGR-1 UCO TRISO fuel," Paper 18576, *Proceedings of the 8th International Topical Meeting on High Temperature Reactor Technology (HTR-2016), November 6–10, 2016, Las Vegas, Nevada*.
- [28] Charles A. Baldwin, John D. Hunn, Robert N. Morris, Fred C. Montgomery, G. W. Chinthaka Silva, and Paul A. Demkowicz, "First Elevated Temperature Performance Testing of Coated Particle Fuel Compacts from the AGR-1 Irradiation Experiment," *Nuclear Engineering and Design*, Vol. 271, 2014, pp. 131–141.
- [29] Robert N. Morris, Paul A. Demkowicz, John D. Hunn, Charles A. Baldwin, and Edward L. Reber, "Performance of AGR-1 High Temperature Reactor Fuel during Post-irradiation Heating Tests," *Nuclear Engineering and Design*, Vol. 306, 2016, pp. 24–35.
- [30] W. Schenk, G. Pott, and H. Nabilek, "Fuel accident performance testing for small HTRs," *Journal of Nuclear Materials*, Vol. 171, 1990, pp. 19–30.

-
- [31] David A. Petti, John T. Maki, Paul A. Demkowicz, and Richard R. Hobbins, "TRISO-coated Particle Fuel Performance," In R. J. M. Konings (ed.), *Comprehensive Nuclear Materials*, Vol. 3, 2012, pp. 151–213.
- [32] Robert N. Morris, John D. Hunn, Charles A. Baldwin, Fred. C. Montgomery, Tyler Gerczak, and Paul A. Demkowicz, "Initial Results from Safety Testing of US AGR-2 Irradiation Test Fuel," *8th International Topical Meeting on High Temperature Reactor Technology (HTR-2016), November 2016, Las Vegas, Nevada*.
- [33] M. Phelip, I. Kadarmetov, D. Petti, H. Nabielek, K. Verforndern, and T. Abram, "TRISO Particle Fuel Performance Code Benchmarking Activities Performed Under The IAEA 6th Coordinated Research Program On Advances In HTGR Fuel Technology," *IAEA Technical Meeting on the Current Status and Future Prospects of Gas Cooled Reactor Fuels, Vienna Austria, June 14–16, 2004*.
- [34] Generation IV International Forum, "Project Arrangement for the VHTR Fuel and Fuel Cycle Project Management Board," GIF/VHTR/FFC/2012/000, April 2012.
- [35] Blaise P. Collin, David A. Petti, Paul A. Demkowicz, and John T. Maki, "Comparison of silver, cesium, and strontium release predictions using PARFUME with results from the AGR-1 irradiation experiment," *Journal of Nuclear Materials*, Vol. 466, 2015, pp. 426–442.
- [36] Blaise P. Collin, David A. Petti, Paul A. Demkowicz, and John T. Maki, "Comparison of fission product release predictions using PARFUME with results from the AGR-1 safety tests," *Nuclear Engineering and Design*, Vol. 301, 2016, pp. 378–390.
- [37] International Atomic Energy Agency, *Fuel performance and fission product behaviour in gas cooled reactors*, IAEA-TECDOC-978, November 1997.